# PRECISION LINEAR FLEXURE BEARING CARTRIDGE

Peckham Engineering and Tool
1151 Fifth Street
Manhattan Beach, CA 90266

April 1994

**DTIC SELECTE NOV.07 1995 B**

*19951106 064*

Final Report

**WARNING** - This document contains technical data whose
export is restricted by the Arms Export Control Act (Title 22,
U.S.C., Sec 2751 et seq.) or The Export Administration Act
of 1979, as amended (Title 50, U.S.C., App. 2401, et seq.).
Violations of these export laws are subject to severe criminal
penalties. Disseminate IAW the provisions of DoD Directive
5230.25 and AFI 61-204.

**DESTRUCTION NOTICE** - For classified documents, follow the procedures in DoD 5200.22-M, Industrial Security Manual,
Section II-19 or DoD 5200.1-R, Information Security Program Regulation, Chapter IX. For unclassified, limited documents, destroy
by any method that will prevent disclosure of contents or reconstruction of the document.

DTIC QUALITY INSPECTED 8

# PHILLIPS LABORATORY
## Space and Missiles Technology Directorate
## AIR FORCE MATERIEL COMMAND
## KIRTLAND AIR FORCE BASE, NM 87117-5776

UNCLASSIFIED

# AD NUMBER

AD- B204595

# NEW LIMITATION CHANGE

TO

**DISTRIBUTION STATEMENT A -**
Approved for public release; Distri-
bution unlimited.

Limitation Code: 1

FROM

DISTRIBUTION STATEMENT  -

Limitation Code:

# AUTHORITY

Janet E. Mosher, Phillips Lab., Kirtland AFB, N.M.

# THIS PAGE IS UNCLASSIFIED

PL-TR-94-1112
This final report was prepared by Peckham Engineering and Tool, Manhattan Beach, CA under
Contract F29601-93-C-0103 Job Order, 21021002, with Phillips Laboratory, Kirtland Air Force
Base, New Mexico. The Laboratory Project Officer-in-Charge was Capt Jeffrey Wiese, (VTPT).

When Government drawings, specifications, or other data are used for any purpose other than in
connection with a definitely Government-related procurement, the United States Government
incurs no responsibility or any obligation whatsoever. The fact that the Government may have
formulated or in any way supplied the said drawings, specifications, or other data, is not to be
regarded by implication, or otherwise in any manner construed, as licensing the holder, or any
other person or corporation; or as conveying any rights or permission to manufacture, use, or sell
any patented invention that may in any way be related thereto.

This report has been authored by a contractor of the United States Government. Accordingly, the
United States Government retains a nonexclusive royalty-free license to publish or reproduce the
material contained herein, or allow others to do so, for the United States Government purposes.

This report contains proprietary information and shall not be either released outside the
government, or used, duplicated or disclosed in whole or in part for manufacture or procurement,
without the written permission of the contractor. This legend shall be marked on any
reproduction hereof in whole or in part.

If your address has changed, if you wish to be removed from the mailing list, or if your
organization no longer employs the addressee, please notify PL/VTPT, 3550 Aberdeen Ave SE,
Kirtland AFB, NM 87117-5776 to help maintain a current mailing list.

This report has been reviewed and is approved for publication.

FOR THE COMMANDER
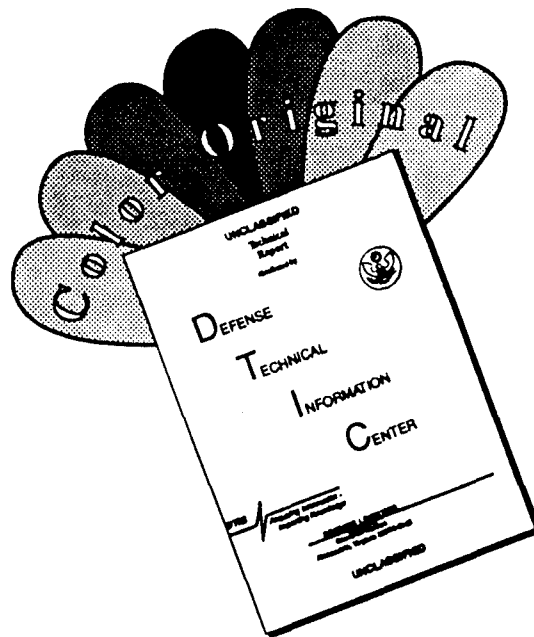
JEFFREY WIESE, Capt, USAF
Project Officer


DAVID KRISTENSEN, Lt Col, USAF       HENRY L. PUGH, JR., Col, USAF
Chief, Space Power and Thermal        Director of Space and Missiles Technology
Management Division


_____DO NOT RETURN COPIES OF THIS REPORT UNLESS CONTRACTUAL
OBLIGATIONS OR NOTICE ON A SPECIFIC DOCUMENT REQUIRES THAT IT BE
RETURNED.

# DISCLAIMER NOTICE

The following notice applies to any unclassified (including originally classified and now declassified) technical reports released to "qualified U.S. contractors" under the provisions of DoD Directive 5230.25, Withholding of Unclassified Technical Data From Public Disclosure.

<u>NOTICE TO ACCOMPANY THE DISSEMINATION OF EXPORT-CONTROLLED TECHNICAL DATA</u>

1. Export of information contained herein, which includes, in some circumstances, release to foreign nationals within the United States, without first obtaining approval or license from the Department of State for items controlled by the International Traffic in Arms Regulations (ITAR), or the Department of Commerce for items controlled by the Export Administration Regulations (EAR), may constitute a violation of law.

2. Under 22 U.S.C. 2778 the penalty for unlawful export of items or information controlled under the ITAR is up to two years imprisonment, or a fine of $100,000, or both. Under 50 U.S.C., Appendix 2410, the penalty for unlawful export of items or information controlled under the EAR is a fine of up to $1,000,000, or five times the value of the exports, whichever is greater; or for an individual, imprisonment of up to 10 years, or a fine of up to $250,000, or both.

3. In accordance with your certification that establishes you as a "qualified U.S. Contractor", unauthorized dissemination of this information is prohibited and may result in disqualification as a qualified U.S. contractor, and may be considered in determining your eligibility for future contracts with the Department of Defense.

4. The U.S. Government assumes no liability for direct patent infringement, or contributory patent infringement or misuse of technical data.

5. The U.S. Government does not warrant the adequacy, accuracy, currency, or completeness of the technical data.

6. The U.S. Government assumes no liability for loss, damage, or injury resulting from manufacture or use for any purpose of any product, article, system, or material involving reliance upon any or all technical data furnished in response to the request for technical data.

7. If the technical data furnished by the Government will be used for commercial manufacturing or other profit potential, a license for such use may be necessary. Any payments made in support of the request for data do not include or involve any license rights.

8. A copy of this notice shall be provided with any partial or complete reproduction of these data that are provided to qualified U.S. contractors.

<u>D E S T R U C T I O N     N O T I C E</u>

For classified documents, follow the procedures in DoD 5200.22-M, Industrial Security Manual, Section II-19 or DoD 5200.1-R, Information Security Program Regulation, Chapter IX. For unclassified, limited documents, destroy by any method that will prevent disclosure of contents or reconstruction of the document.

# DRAFT SF 298

| 1. Report Date (dd-mm-yy) April 1994 | 2. Report Type Final | 3. Dates covered (from... to ) 1/93 TO 3/94 | | |
|---|---|---|---|---|
| 4. Title & subtitle<br><br>Precision Linear Flexure Bearing Cartridge | | 5a. Contract or Grant # F29601-93-C-0103 | | |
| | | 5b. Program Element # 62601F | | |
| 6. Author(s) | | 5c. Project # 2102 | | |
| | | 5d. Task # 10 | | |
| | | 5e. Work Unit # 02 | | |
| 7. Performing Organization Name & Address Peckham Engineering and Tool 1151 Fifth Street Manhattan Beach, CA 90266 | | 8. Performing Organization Report # | | |
| 9. Sponsoring/Monitoring Agency Name & Address Phillips Laboratory 3550 Aberdeen Ave SE Kirtland AFB, NM 87117-5776 | | 10. Monitor Acronym | | |
| | | 11. Monitor Report # PL-TR-94-1112 | | |
| 12. Distribution/Availability Statement<br>Distribution authorized to DoD components only; Proprietary Information;April 1994. Other requests shall be referred to AFMC/STI. | | | | |
| 13. Supplementary Notes | | | | |

**14. Abstract** Morphological analysis of thermodynamic machines shows that there are three major elements that are utilized by every type of engine; thermal energy recovery heat exchangers (recuperates, regenerators); electromechanical energy convertors (linear or rotary moving coil, moving iron, or moving magnet motors/alternators: and bearing systems (fluid, rolling element, electromagnetic, flexure). One particularly interesting class of engine is based on resonant linear reciprocating mechanisms, the most typical using flexure bearings and a moving coil linear motor/alternator. While all of the components could be improved, the linear flexure bearing system is the one most in need of refinement. This Phase I SBIR program was conducted (1) to define the basic research and development necessary for the development of a universally applicable linear flexure bearing cartridge technology, (2) to demonstrate the feasibility of critical elements and processes, and (3) to prepare a Phase II proposal for fabricating complete prototype cartridges.

**15. Subject Terms** engine, motor, coil linear motor, linear flexure bearing cartridge

| Security Classification of | | | 19. Limitation of Abstract | 20. # of Pages | 21. Responsible Person (Name and Telephone #) |
|---|---|---|---|---|---|
| 16. Report Unclassified | 17. Abstract Unclassified | 18. This Page Unclassified | Limited | 84 | Capt Jeffrey Wiese (505) 846-2686 |

## GOVERNMENT PURPOSE LICENSE RIGHTS
## (SBIR PROGRAM)

**Contract Number: F29601-93-C-0103**
**Contractor: Peckham Engineering and Tool**
      **Manhattan Beach, CA**

## TABLE OF CONTENTS

## TABLE OF CONTENTS

List of Figures

## TABLE OF CONTENTS

List of Figures (continued)

## PRECISION LINEAR FLEXURE BEARING CARTRIDGE
PHASE I FINAL REPORT

### I.0 IDENTIFICATION AND SIGNIFICANCE OF TECHNOLOGY

Morphological analysis of thermodynamic machines shows that there are three major elements that are utilized by every type of engine: thermal energy recovery heat exchangers (recuperators, regenerators); electromechanical energy convertors (linear or rotary moving coil, moving iron, or moving magnet motors/alternators); and bearing systems (fluid, rolling element, electromagnetic, flexure)[1][1] . One particularly interesting class of engine is based on resonant linear reciprocating mechanisms, the most typical using flexure bearings and a moving coil linear motor/alternator. While all of the components could be improved, the linear flexure bearing system is the one most in need of refinement[2,3]. This Phase I Small Business Innovative Research (SBIR) program was conducted (1) to define the basic research and development (R&D) necessary for the development of a universally applicable linear flexure bearing cartridge technology, (2) to demonstrate the feasibility of critical elements and processes, and (3) to prepare a Phase II proposal for fabricating complete prototype cartridges.

A linear flexure bearing is a frictionless, nonwearing assembly designed as a precision support for a reciprocating member. Figure I-1 depicts a generalized linear flexure bearing configured to support a round shaft concentric within a round bore. A typical bearing consists of the outer rim, the inner rim, and the flexure diaphragm(s). The outer rim provides the external mounting surfaces and attachment provision(s) plus the built-in edge constraint and axial spacing for the outer edge of the flexure diaphragm(s). The inner rim provides the equivalent accommodations and constraints for the inner diameter of the flexure diaphragm(s).

---

[1] *[Bracketed superscript numbers identify references]*
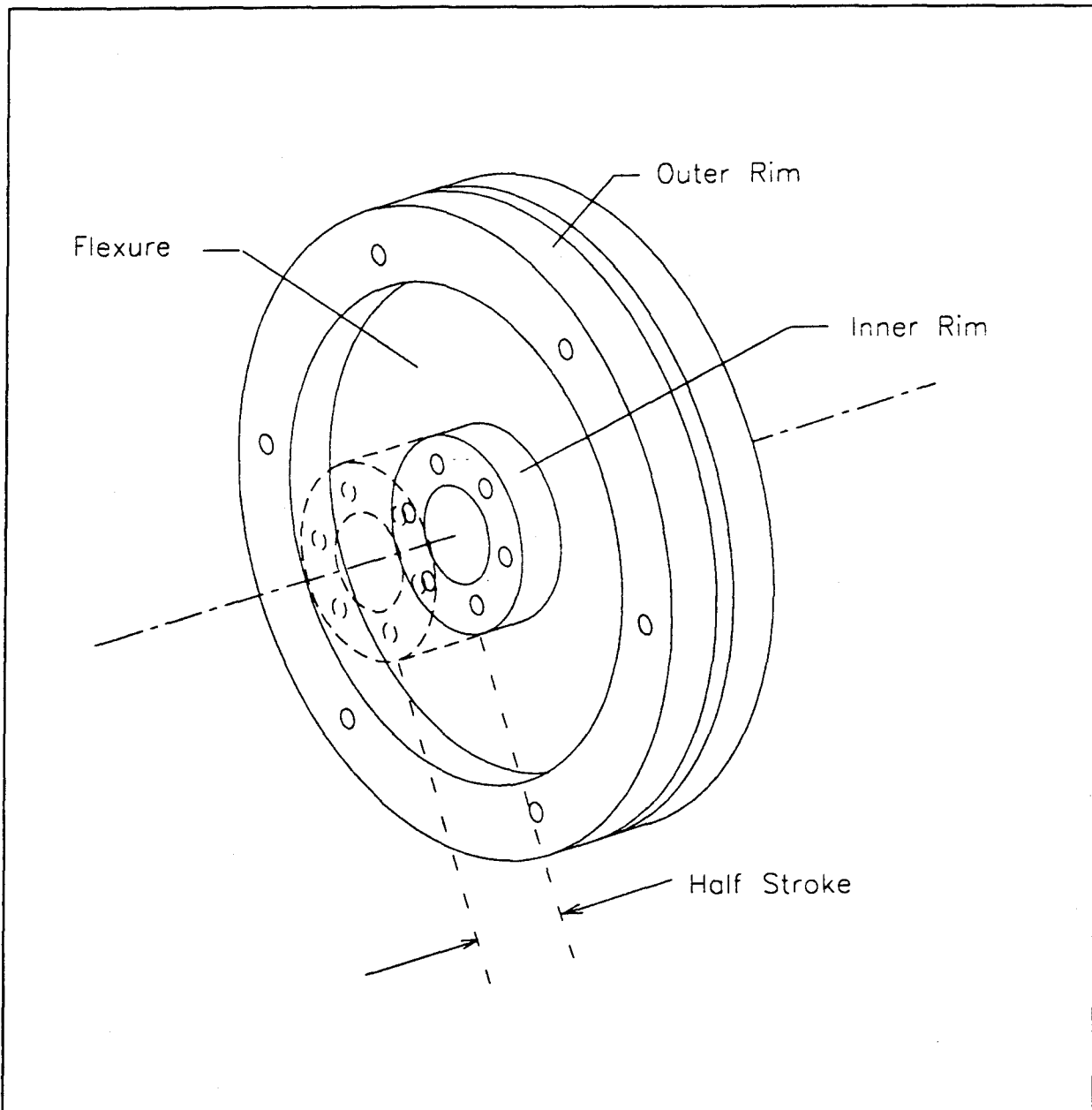
Figure I-1; Generalized Linear Flexure Bearing

In a typical installation, the bearing design requirements will be based on the supported shaft outside diameter (OD) (bearing inside diameter [ID]), the required stroke, the allowable bearing support length, a measure of the bearing precision such as the allowable dynamic concentricity, the required radial support stiffness or spring constant, the operating frequency, the allowable axial spring constant, the operating environment (temperature, vibration, immersion fluid, magnetic field, etc), storage and operating life, and mechanical reliability. For design optimization, it is desirable to minimize the bearing cartridge housing OD, to minimize the cartridge weight, to maximize the ratio of radial spring constant to axial spring constant, and to design the flexure element natural frequencies to nonharmonics of the operating frequency.

While oscillatory rotary flexure bearings are catalogue items (Bendix rotary flexure instrument bearings), linear flexure bearings are all empirically custom designed and developed. The flexure diaphragm configuration is sized to the specific requirements and fabricated by photoetching, electric discharge machining, laser cutting, abrasive water jet cutting, or stamping from spring stock. To provide the concentric linear support, a set of the flexure diaphragms is assembled within the support body bore diameter using spacers, through bolts, special assembly fixtures, and shims. Because of the variability of this process, it is often necessary to disassemble and reassemble the parts in order to achieve the required concentricity. Due to the custom design and complex assembly methods, current linear flexure bearing implementations are not suitable for mass production. Figure I-2 shows typical circular flexure diaphragms
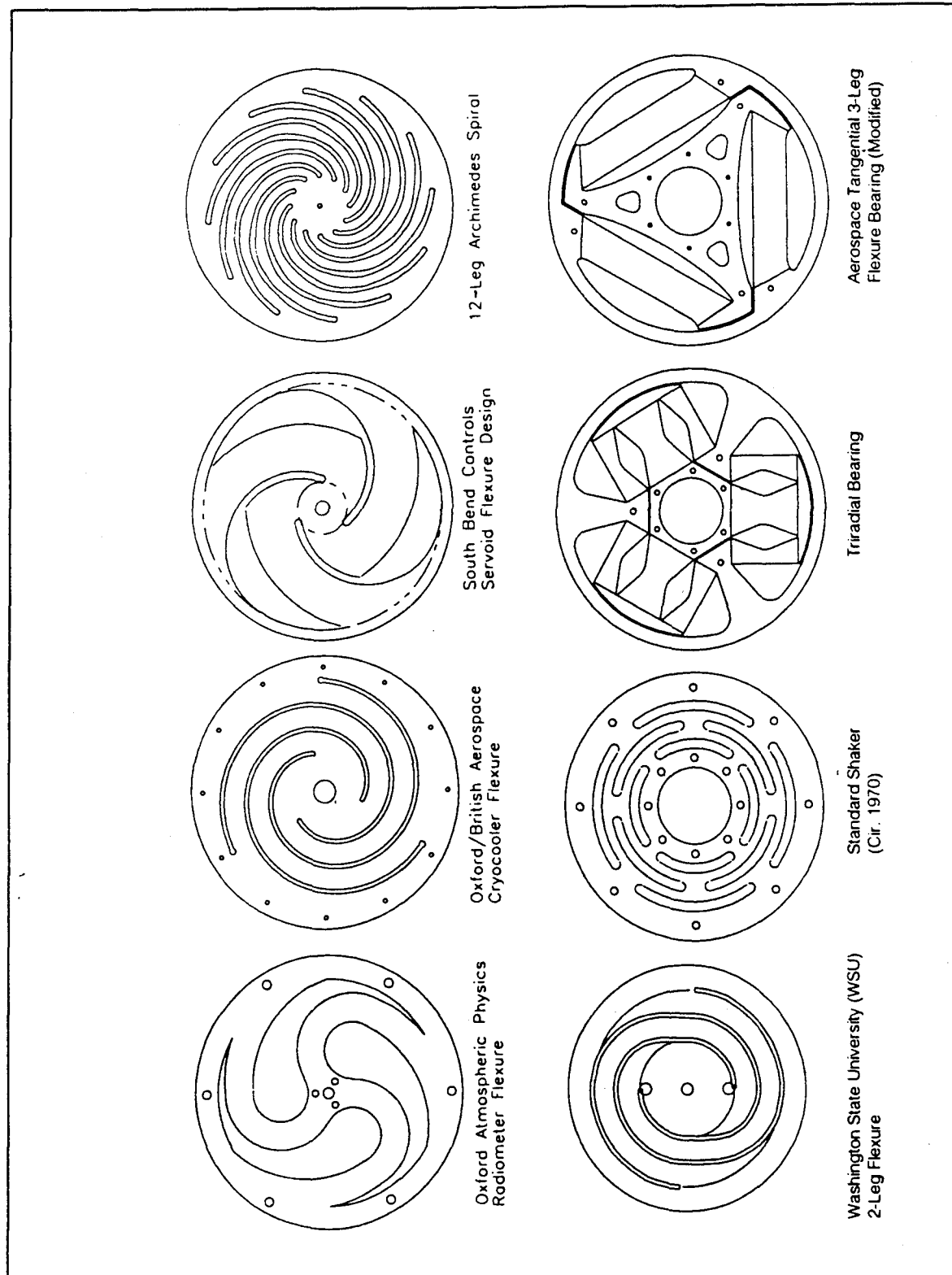
Figure I-2: Typical Flexure Spring Designs

The Oxford Atmospheric Physics Radiometer flexure[4] was the precursor to the Oxford/British Aerospace (Bae) cryocooler flexure[5]. The Oxford/Bae spiral cut flexure diaphragms are fabricated from beryllium copper spring stock by photoetching. For flexure reliability, it is necessary to eliminate any local edge stress risers caused by the fabrication process. The method utilized to round and polish the edges of the spiral cuts has not been publicly described. Given the narrow gap, it is possible that some form of electropolishing is used. Alternately, the slots could be hand tool deburred and polished using die making techniques. The flexures are installed with spacers and axial screws at the inner and outer circumferences. Alignment of the moving close clearance piston or displacer must be accomplished with shims and/or special tooling. The alignment is maintained by the friction forces created by the circumferentially located screws used to mount the flexures. It is apparent that the processes used in fabricating and installing the Oxford/Bae cryocooler flexure are labor intensive, of variable quality, and prone to the creation of built-in stresses which could shift the alignment while subjected to the many billions of cycles of operation.

The Servoid flexure is a South Bend Controls proprietary configuration[6]. The "Doily Cut" flexure was the standard design used in electrodynamic shakers in the 1970's. It has subsequently been replaced with a three- dimensional support such as shown in Figure I-3. This three- dimensional support does exhibit long life and high reliability; however, it is not suitable for maintaining close radial tolerances. The Washington State University (WSU) 2-leg flexure was developed as part of a Stirling cycle heart pump program[7]. The TriRadial flexure configuration is an alternate examined as part of this effort which did not favorably compare with either the Oxford/Bae or the Aerospace 3-Leg Tangential[2].
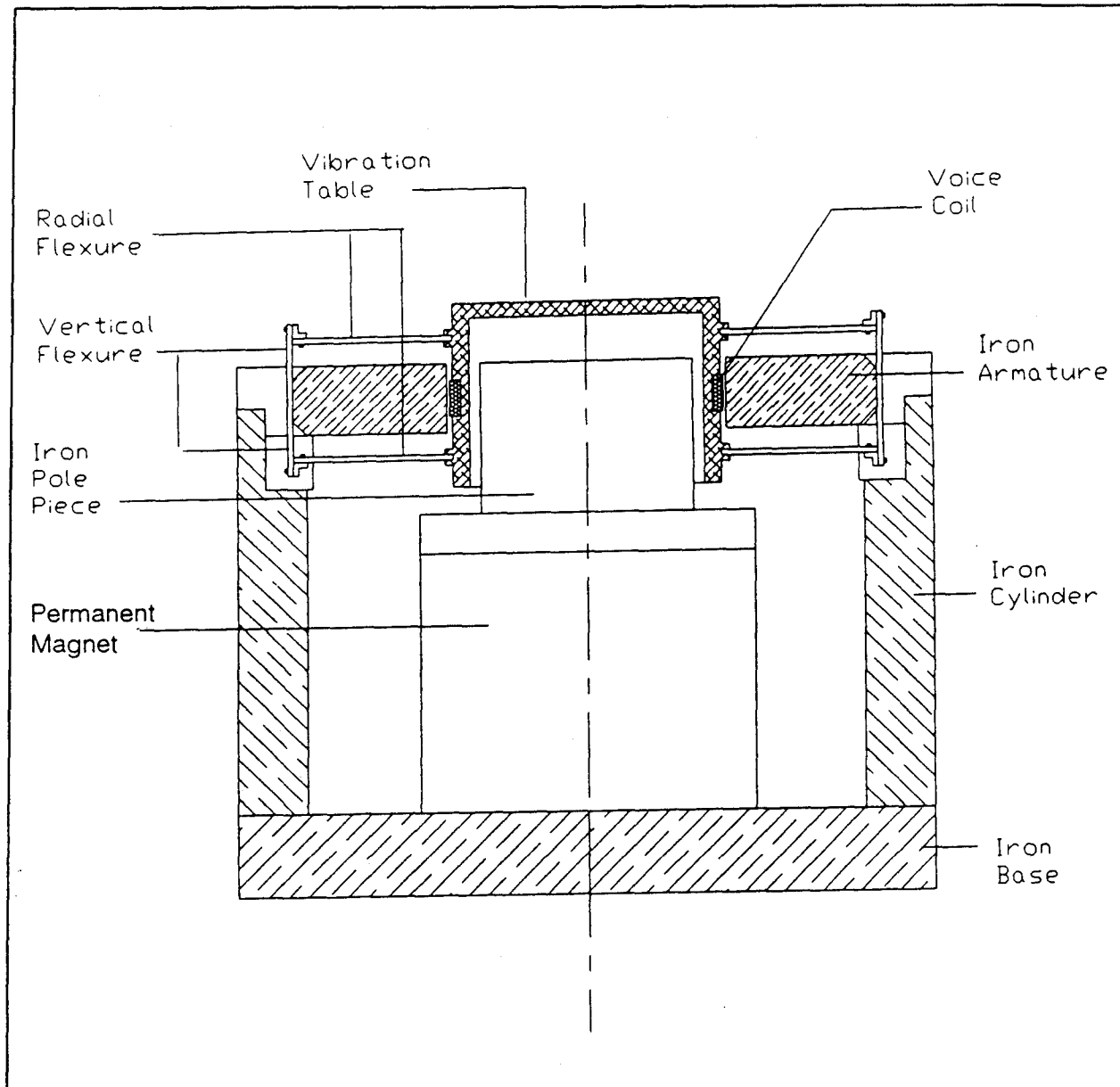
Figure I-3; Modern Shaker Flexure Bearing

I.1 Flexure Diaphragm Geometry

The design of a linear flexure bearing diaphragm to meet a specific requirement involves a trade optimization of a number of variables. The flexure spring material selected defines the allowable maximum design stress, given the stock thickness, temper, "grain" direction, and fabrication processes. The cut diaphragm flexure size and pattern, with defined edge constraints, will determine the maximum static stress, given the maximum deflection, stock thickness, and material properties. Given a matrix of competitive alternatives which meet the material and design limitations, the "best" design will have the highest radial stiffness at the fully deflected condition[2].

For a given size, and assuming equal flexure leaf "length," increasing the number of leafs will neither increase the allowable stroke nor greatly reduce the axial spring constant. The radial stiffness, or spring constant, however, will be significantly lowered as the number of leafs increase. Equally spaced three leg designs prove to be best. Spiral cut flexure diaphragms are the principal configuration currently being utilized in the design of linear drive compressors and wave generators. This particular choice is probably due to the success of the Oxford design.

Wong et al.[2] documented the advantages of the Tangential 3-Leg configuration over the spiral cut. A significant portion of the Phase I effort was to expand upon these studies to explicitly demonstrate the potential advantages of the Tangential 3-Leg configuration. Figure I-4 shows a representative geometrical description that was used to characterize the Tangential 3-Leg configuration. By parametrically varying the dimensions $\theta$, W, and $h_t$ where $h_t$ is the flexure material thickness, the flexure response was characterized. To limit this parametric analysis to a level of effort commensurate with the scope of Phase I, the dimensions
$r_c$ = 4.90 cm
H  = 4.25 cm
$r_t$ = 0.00 cm
$\phi$  = 30°
$\theta$ = 90°, 105°, 120°
W = 1.00, 1.25, 1.50 cm
$h_t$ = 0.125, 0.1875, 0.250 mm
were selected.
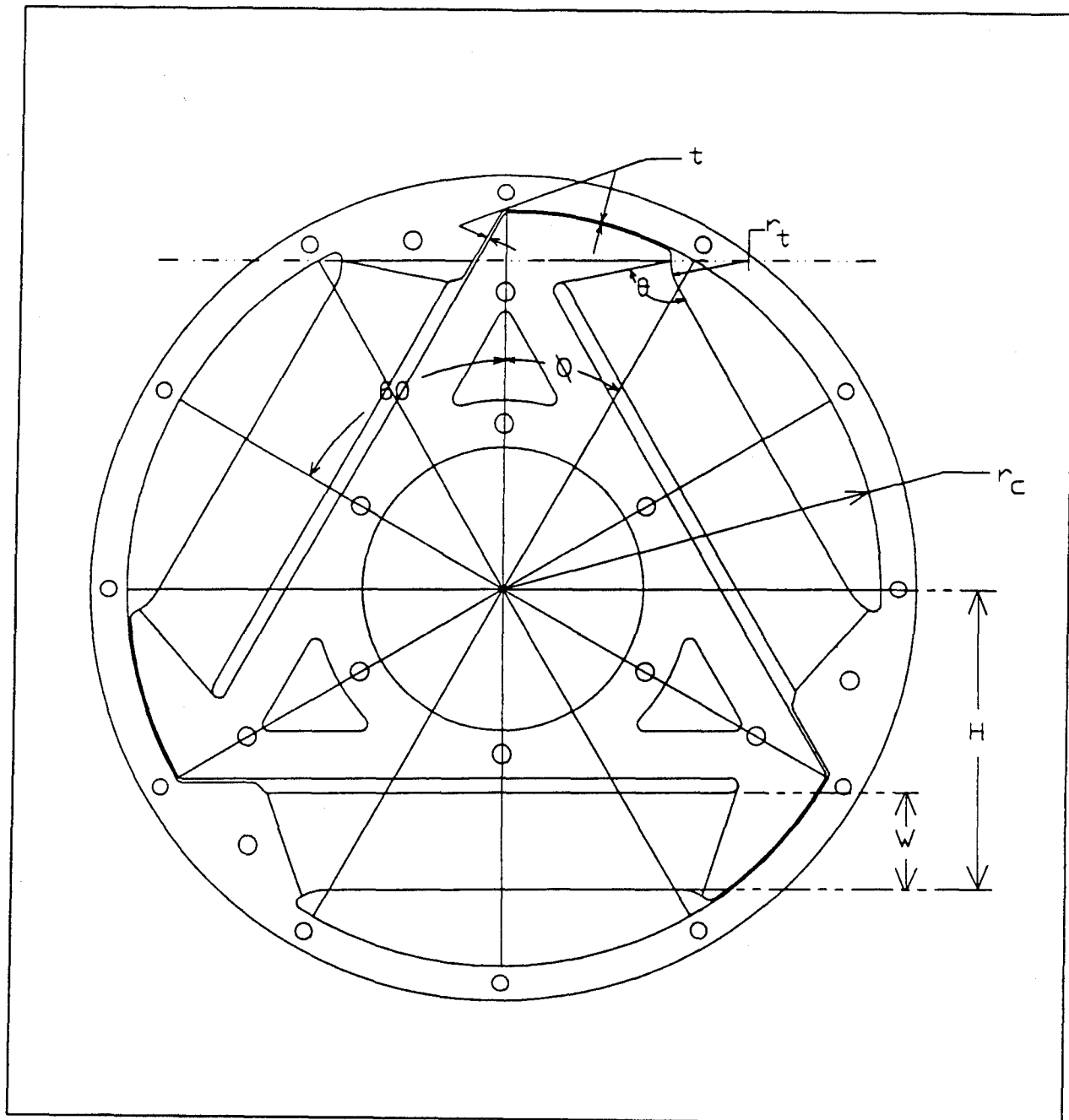
Figure I-4; Representative Tangential 3-Leg Geometry

I.2 Flexure Diaphram Material

To select a diaphragm flexure spring material, it is necessary to know the anticipated number of operating cycles. As a goal, a 10-year operational life at 60 cycles per second would seem acceptable. Such a goal translates to approximately $20 \times 10^9$ reversing cycles. There is little material cyclic fatigue data beyond $10^7$ cycles; however, several materials exhibit an "infinite" fatigue life at approximately $10^6$ cycles. It is important to note that this "limit" is usually the 50% probability of failure line, although some sources also include the 10% and 90% probability of failure data. When reviewing the data, it is also important to be aware of the "type" of cyclic stress being reported, tensile, reversing bending, torsion, etc.

Candidate diaphragm spring materials include beryllium copper, stainless steel, and titanium. Manufacturer's data on the fatigue properties of these materials was obtained. The data was checked with that reported in the standard references and found to be acceptable. Due to the large number of variables such as surface finish, edge finish, specimen flatness, specimen thickness tolerance, specimen axis orientation to strip axis, material heat treatment, material quality control, etc., involved in fatigue life testing, it would be anticipated that there would be some variation in the mean failure curve and its standard deviation as reported by various sources. To minimize the influence of these variables, it is important to select a reliable, consistent source. Wohler S-N (Stress - Number of Load Cycles) curves for 50% failure of the beryllium copper alloys and the titanium alloy strip under reverse bending were reviewed. None of these materials exhibited an infinite cycle fatigue stress limit. The S-N data for the stainless steels, however, do exhibit an effectively infinite cyclic fatigue stress limit. Figure I-5 presents a Wohler S-N plot for 10%, 50%, and 90% fracture probability of a Uddeholm 716 stainless steel strip in tensile loading for two different conditions, with polished edge and "as blanked" edge[8]. It is often necessary to provide electrical power to the linear motor moving coil via a flexible electrical conductor. Analysis has shown that the electrical resistance of the stainless steel flexures is low enough to be acceptable for such an application. There appears to be no reason, therefore, to use either beryllium copper or Ti-6Al-4V as a diaphragm material for linear flexure bearings.
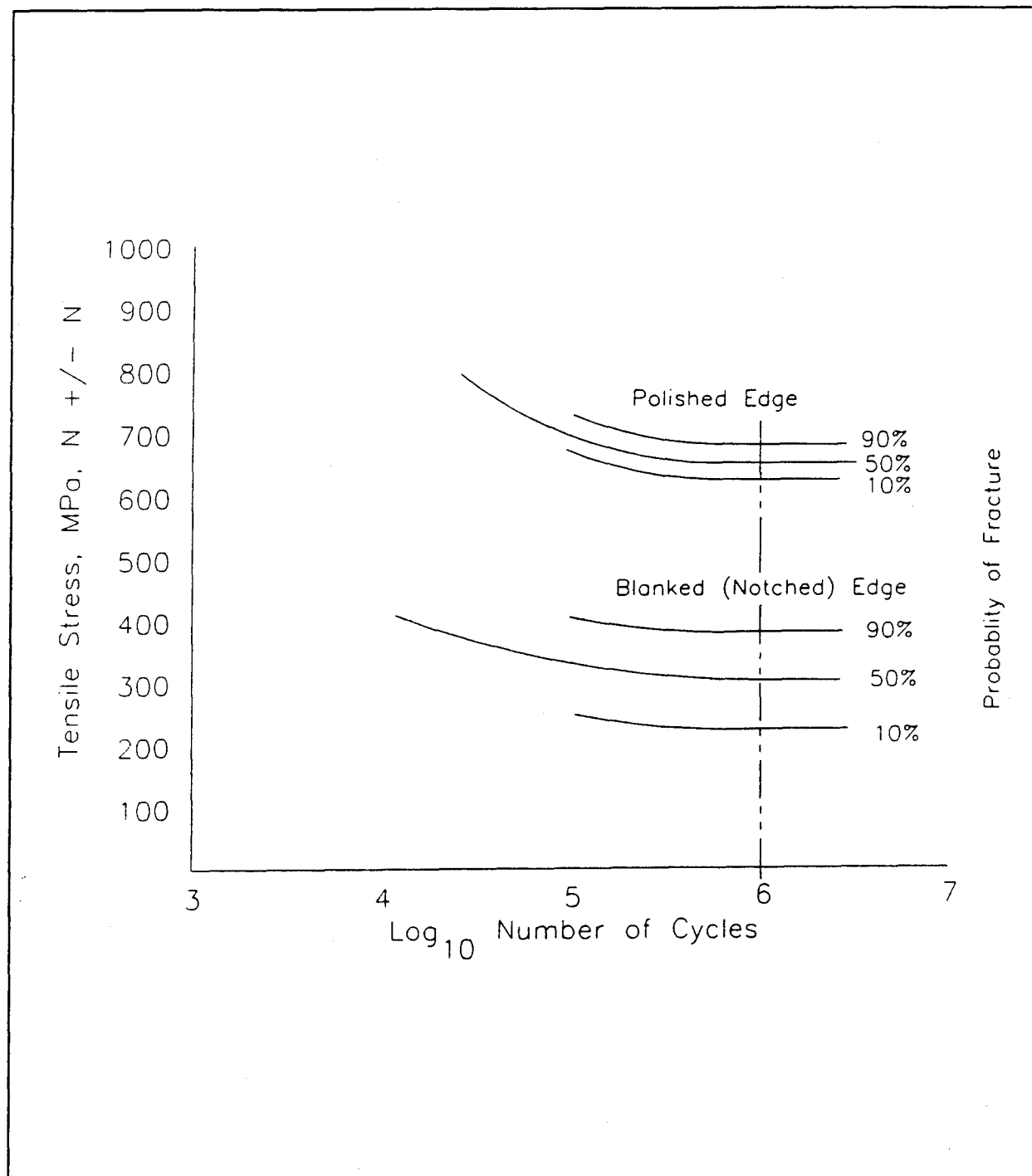
Figure I-5; Uddeholm 716 S-N Curves

S-N reverse bending plots were not available, however, the following information was provided in the accompanying text: "... for flapper valve steel ... the fatigue properties are strongly related to the ultimate tensile strength... The 'Fatigue limit ratio' is defined as the stress amplitude at the fatigue limit divided by the ultimate tensile strength. Statistical analysis ... indicate strongly a constant, strength independent standard deviation from batch to batch. Stainless 716: ultimate tensile - 1810 MPa, reverse bending fatigue limit ratio - 0.41, tensile fatigue limit ratio - 0.33. Standard deviation - 35 MPa."[8] This material exhibits an effectively infinite cycle fatigue life limit after $10^6$ cycles. Since the 90%, 50%, and 10% probability of fracture curves are provided, it is possible to estimate an infinite cycle fatigue limit stress for a very low probability of failure, such as 0.001%, by assuming that the probability of fracture at the infinite cycle regime is normally distributed. The literature suggests that the assumption of a normal distribution for the probability of fracture about the mean (50%) fracture stress is reasonable. Experimental confirmation would be required to validate the final design, but considering the variations in the S-N curves as a function of strip thickness, orientation of the major axis of the sample to the long axis of the strip, edge finishes, surface finishes, heat treatment, etc., including a reasonable design margin should suffice. Note that bending perpendicular to the strip grain axis is preferred to bending across the grain axis.

The polished edges (external edges) on the test specimens used by Uddeholm in the bending and tensile fatigue life testing were obtained by barrel tumbling with water and aluminum oxide (2-10 mm grains) for 10hrs. The edges were inspected at 100x magnification to confirm the rounding and polishing of the edges. It was noted that the rounding and polishing of the edges of internal holes could not be adequately processed by the standard barrel tumbling process. Centrifugal Barrel Finishing (CBF), however, can polish the edges of small slots[9]

For effectively infinite life, the reverse bending fatigue strength design will be selected down four standard deviations from the 50% failure rate value. A standard deviation is ~5% of the 50% failure rate value. To account for inaccuracies in the stress analysis, manufacturing variations, and fabrication induced stress risers, a design margin of 50% is applied. The allowable design stress is thus 0.41 x 0.8 x 0.5 x 1810 MPa = 296 Mpa.

## II.0 PHASE I OBJECTIVES

Table II-1 summarizes the Phase I program by task.

TABLE II-1;

| Task | Description | Result | Comment |
|------|-------------|--------|---------|
| Program Plan Revision | Provides the opportunity to revise the program plan to include aspects of the technology which become evident between the proposal preparation and contract award. | Limiting the metallurgical bonding process to diffusion welding over-constrained the program. To correct this deficiency, evaluation of brazing, soldering, and adhesive bonding alternatives were added to the program plan. | This task is essential for the successful completion of a R&D activity. The changes in scope (but not in funding) resulted in a Phase I technology demonstration which can be transferred to a meaningful Phase II program. |
| Literature Survey | Delve into the relevant technical literature thoroughly focused on the Phase I R&D activities and tasks. | Literature survey disclosed that common fatigue testing techniques were not suitable for obtaining numerous rapid S-N of cycles data as required by program. Several alternate approaches were identified as acceptable. | With a materials and processes intensive research program, a continued emphasis on reviewing the relevant contemporary technical literature is imperative. There is insufficient discretionary funding available to a small company to complete this task prior to the contract award. |
| Programmatic Support | Covers the administrative functions which are unique to the contracted effort. | Of all the activities included within this task, the coordination of the billing and reimbursement was more time consuming than anticipated. Instruction on completing and transmitting DD 250 forms was provided to expedite this process. | Initially, the transmittal and processing of the DD 250 forms through the various approval offices resulted in a funding delay that caused a slippage in the completion of the Phase I effort. |
| Technical Direction | Responsible for all aspects of the technical direction of the program. | A review of the technical papers obtained in the literature survey necessitated the expansion of the scope of several tasks. | Principal Investigator must recognize when redirection is needed and know how to efficiently implement the required changes. |

TABLE II-1; CONTINUED

| Task | Description | Result | Comment |
|------|-------------|--------|---------|
| Conceptual Design | Prepare a conceptual design of the precision linear flexure bearing cartridge considering diaphragm configuration(s), material and processes, and methods of installation. | Several alternative configurations were synthesized and evaluated. It was concluded that the Aerospace Tangential 3-Leg Flexure diaphragm needed to be rigidly bonded to the outer rim and to the inner spider in order to properly function. The spiral configurations will properly function if only mechanically supported at the inner and outer edges. | The addition of electrically insulating inner and outer rims will allow the use of the flexure to also transmit power to the moving coil, thus simplifying the total installation. |
| Material Selection | Identify suitable materials and sources for same. Define the material properties to be used in the design analysis. Delineate methods for inspection, fabrication, finishing and bonding the cartridge materials. | Determined that Uddeholm 716 is the appropriate material for the flexure diaphragm. Discovered that CBF is an acceptable method for polishing the edges of the flexure. Concluded that diffusion bonded copper plated joints would suffice for the flexure bonding process. Suggested metallurgically bonded zirconia or frit bonded metal rims to provide electrically insulated interface. | Creating an adhering copper flash on the 716 corrosion resistant steel (CRES) proved to be difficult. Standard tank plating processes were inadequate to remove the oxide. A special brush plating process proved successful. Special advanced tank plating processes or a novel "pad" plating concept invented as part of this program are alternatives to be explored during phase II. |
| Processes and Manufacturing Controls | Prepare a preliminary draft of the processes and manufacturing controls document based on the Phase I effort, expanded and completed in Phase II. | Document prepared based on the material selection and test specimen fabrication tasks. Located several grinding machines that can provide the accuracy necessary to meet the required tolerances. | When fully documented in Phase II, this information will constitute the primary technology advance of this R&D program. The techniques will prove useful to devices other than just the flexure bearing. |

TABLE II-1; CONTINUED

| Task | Description | Result | Comment |
|---|---|---|---|
| Flexure Finite Element Analysis (FEA) Trade Study | FEA trade study was conducted comparing the Tri-Radial, the Aerospace asymmetrical Tangential 3-Leg, and 27 variations of a symmetrical Tangential 3-Leg flexure diaphragm. Peak stresses, radial and axial stiffness, and axial rotation versus axial deflection were computed for similar dimensional configurations. | The FEA showed the superiority of the symmetrical Tangential 3-Leg design over the Tri-Radial and asymmetrical Tangential 3-Leg configurations. Since the asymmetrical Tangential 3-Leg design has previously been shown superior to the spiral configuration, it is concluded that the symmetrical Tangential 3-Leg configuration is the best currently known. | The trade study showed that an optimum flexure-to-boundary angle exists for any given blade width and thickness. Phase II will expand on these studies by considering smaller and larger OD designs, will expand on the parametric optimization, and will prepare a design handbook based on these findings. |
| Precision Linear Flexure Bearing Cartridge Preliminary Design Layout | A preliminary design layout of a typical precision linear flexure bearing cartridge was prepared. The dimensional tolerances specified were consistent with the capabilities of known machines. | Using the geometry of the "best" flexure diaphragm obtained from the FEA trade study together with the results of the material selection and processes and manufacturing controls tasks, a preliminary design layout was prepared. | The preliminary design configuration will be used to detail design and fabricate the "Pathfinder" engineering model early in the Phase II program. |
| Test Specimen Design | The revised test description can be paraphrased as: "Design a uniform built-in beam with centrally load cyclic excitation to evaluate the effect of the manufacturing processes on the basic material properties." | The test specimen was designed to be fatigue tested at frequencies in excess of 100 cycles per second (CPS) (Hertz). | The test specimens were designed to utilize the edge polishing, copper plating, and furnace bonding techniques to be used in Phase II. |

TABLE II-1; CONTINUED

| Task | Description | Result | Comment |
|---|---|---|---|
| Test Fixture Design | Revised task can be paraphrased as: "Design a fatigue test fixture that can rapidly measure the fatigue properties of spring stock and related fabrication techniques." | A novel 2 degree of freedom fatigue testing fixture/machine capable of operating at frequencies up to 250 CPS was designed. Test specimens are driven at their natural frequency, which allows for the high operating frequency. This design was dictated by the extreme acceleration levels resulting from the high frequency. | In essence, the test specimens are the flexures which are supporting the balance mass in a "Frohm" vibration balancing machine. |
| Material Procurement | Procure samples of candidate materials which could be used in the precision linear flexure bearing cartridge and evaluate by fabricating into the fatigue test specimens. | Various thicknesses of Uddeholm 716 CRES spring stock and copper brush plating solutions suitable for flash deposition on 716 were obtained. | All materials are readily available. Additional research is needed in Phase II to explore alternate copper plating solutions and techniques. |
| Test Fixture Fabrication | A test fixture was built to the design described above. The fixture was tested to confirm operation using adhesively bonded test specimens. | The use of the adhesive bonded test specimens also served as a check on the effect of the polishing and plating process. | The fatigue test fixture performed exactly as analyzed. |
| Test Specimen Fabrication | Using the materials procured, the designs created, and processes developed under previous tasks, fabricate sufficient fatigue test specimens to evaluate the suitability of the technology. | The test specimens were successfully fabricated using the technology developed in the previous tasks. Bonding of the copper-plated plated interfaces required the use of a hydrogen atmosphere furnace. | To assure a complete copper interface diffusion bond, it is necessary to fabricate the parts in an extremely clean environment and to minimize the oxide on the surfaces to be joined. |

TABLE II-1: CONCLUDED

| Task | Description | Result | Comment |
|---|---|---|---|
| Specimen Testing | Fatigue flexure test specimens were loaded into the test fixture and electromagnetically excited to a controlled displacement corresponding to the desired stress level. | The specimens were tested at several stress levels. The results confirmed the published Uddeholm fatigue data within the experimental error of the test equipment/procedure. The CBF edge proved successful. The copper bonding process did not adversely affect the material fatigue strength. | The high frequency fatigue testing hardware proved successful, providing the necessary data in a short time. |
| Metallurgical Analysis | Specimen blanks, edge polished flexure specimens, diffusion bonded test specimens, and cyclic tested specimens were subjected to a microscopic metallurgical analysis. | The CBF process produced acceptable polished edges. The brush plated and diffusion bonded copper joint developed an adequately strong interface. | The metallurgical analysis confirmed the acceptability of the critical materials and processes needed for the Phase II program. |
| Phase II Proposal | Prepare a proposal for Phase II. | This document was prepared in conformance with the directions. | The Phase I final report will provide details on the tasks described above. To minimize program disruption, the Phase II award is needed before the Phase I final report is completed. |
| Final Report | Document the results of the Phase I program. | These tables summarize the highlights of the Phase I program. | The Phase I program successfully demonstrated the critical technologies needed for the Phase II program to design, build, and demonstrate the precision linear flexure bearing cartridge. |

## III.0 OVERALL WORK PLAN

The overall (Phase I and II) work plan was structured to design, fabricate, characterize, and life test a suite of representative prototype precision linear flexure bearing cartridges. The representative suite would be sized to span a range of sizes sufficient to establish the credibility of the technology for use in devices ranging from the 10's of watts up to several kilowatts in power input/output (~5 to ~15 cm. OD). The materials, processes, and tooling used in fabricating the prototype units would be selected to simulate that required for large scale production with sufficient fidelity to allow for creditable extrapolation to production hardware characteristics and costs. To allow for this extrapolation, several different diameter designs spanning the range of interest would be tooled, fabricated, characterized, and life tested. Analogous to roller bearing technology, the cartridges would be modularized so that multiples could be used to obtain various load carrying capacity. The dimensional accuracy of the cartridges would be controlled to the tolerances required to allow their use without the need to selectively fit or shim in order to maintain the narrow concentric clearances required by noncontacting gaseous gap seals (<0.005 +/- 0.001 mm radial clearance). The Phase I effort defined the basic cartridge configuration, experimentally evaluated the more critical fabrication techniques, and conducted a parametric finite element stress analysis of typical flexure.

As an alternative to the present method of fabricating and assembling linear flexure bearings, the concept of the "precision linear flexure bearing cartridge" is proposed. This component is an analog of the frictionless rotating shaft ball bearing cartridge. The dimensional control of the axial position of the supported reciprocating shaft is established by the tight tolerance internal and external mounting diameters. Figure III-1 shows a typical configuration. A pair of such cartridges creates a total bearing support system. The ID and OD of the cartridge are ground to the final dimensions prior to the wire electric discharge machining (EDM) which separates the central spider with its internal shaft support from the external rim.
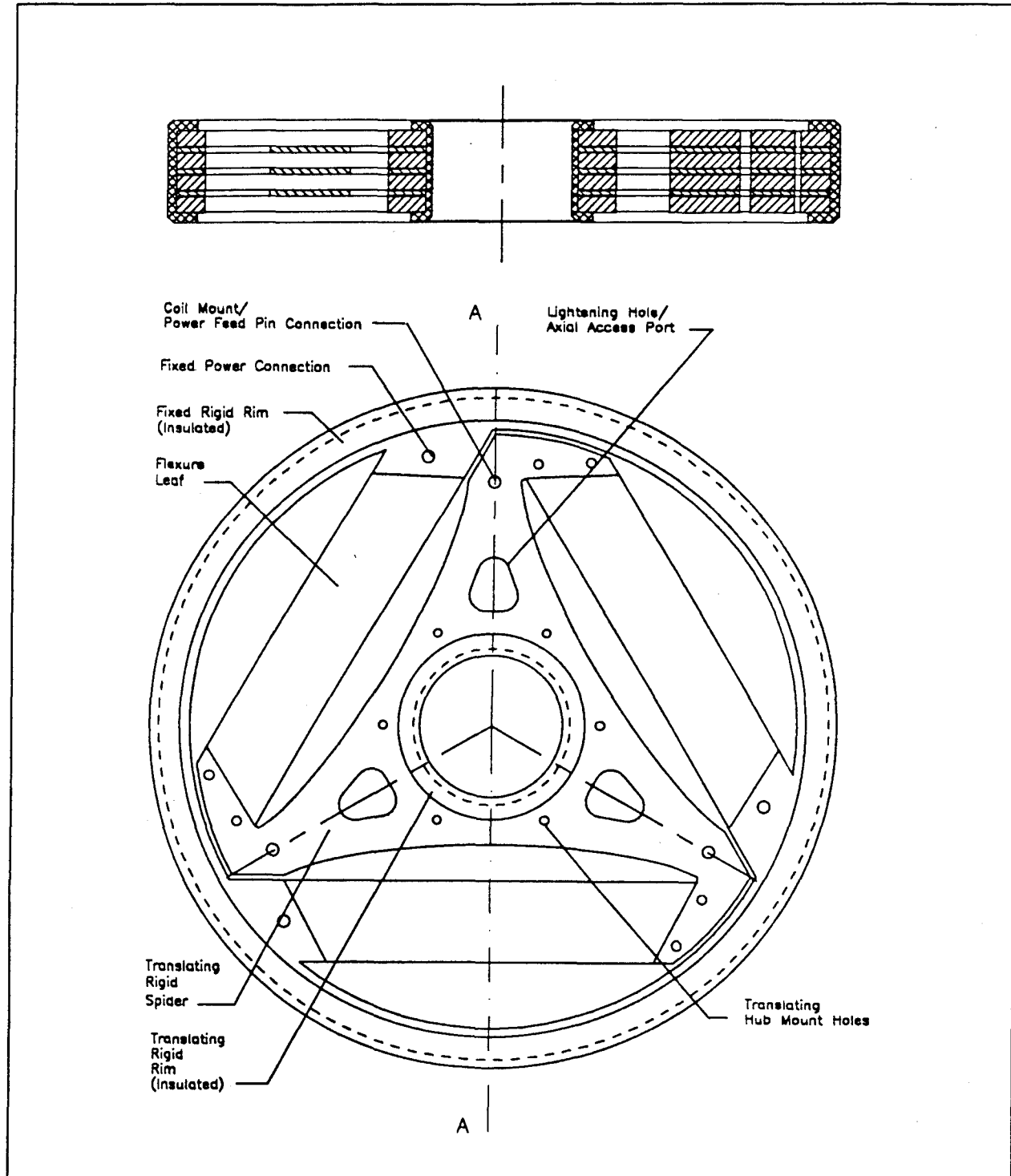
Figure III-1;  Precision Linear Flexure Bearing Cartridge

The following fabrication process will be used to make the flexure element parts:

1. Flexure diaphragm segments will be cut from Uddeholm 716 thin spring stock ribbon, oriented so that the active flexure leaf is aligned with the ribbon grain (Figure III-2).

2. Bearing spacer/doublers will be cut from Uddeholm 716 thick spring stock ribbon. The orientation/aligned with the ribbon grain is not critical (Figure III-2).

3. The cut parts will be deburred and edge polished using the Harper Surface Finishing Systems "Harperizing" CBF process[9].

For the Phase II "Pathfinder" segment, the parts will be cut by photoetch techniques. For the Phase II prototype segment, dies will be fabricated and the parts will be cut by stamping. The cut parts will be shipped to the "Harperizing" vendor. When returned from the vendor, the edge of the polished parts will be inspected, cleaned, and stored in an appropriate protective environment until needed for the subsequent copper plating process. The "Harperizing" process was selected over the "extrusion" edge polishing process originally described in the Phase I proposal due to the ability of the process to produce a satisfactorily polished edge at a much lower unit cost.
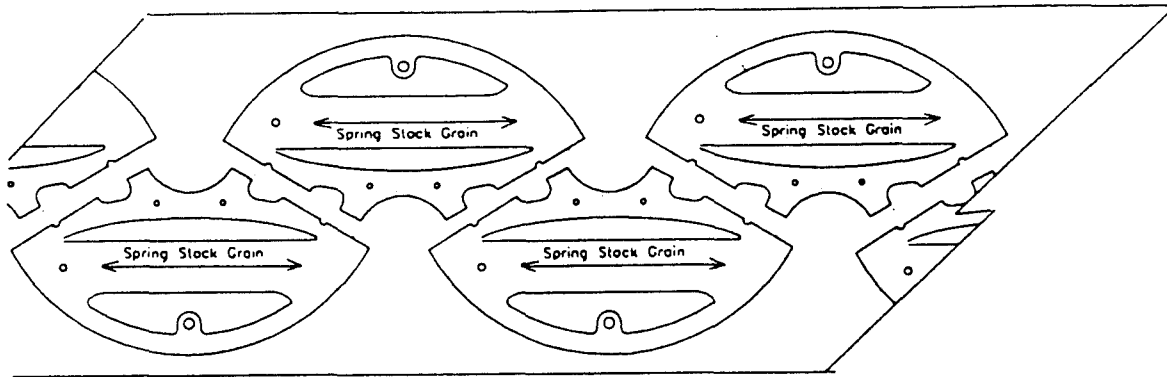
Cut Flexure Segments From Spring Stock

Cut Flexure Doublers From Thick Spring Stock
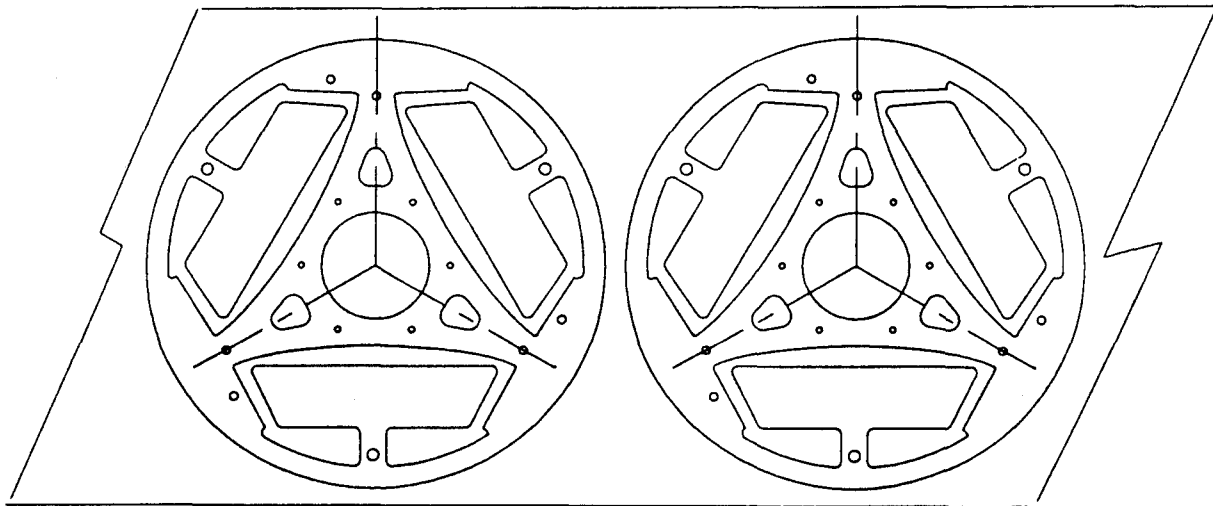
Figure III-2; Flexure Diaphragm Segment/Spacer Doubler Stamping

In Phase I, the required copper flash pattern was satisfactorily electrodeposited on the test samples by two different processes, tank plating and brush plating. In Phase II, an alternate process that mixes the best features of these two processes will also be investigated as part of the effort to minimize fabrication cost. In any process, the active surfaces of the flexure segment must be protected during the plating process to assure that copper is not deposited on the flexing blade.

With tank plating, it is necessary to mask the active blade portion to protect it from being affected in the subsequent electrolytic bath processes. The edge-polished and masked flexure segments are loaded into an electrolytic bath where the exposed surfaces are anodically cleaned (deoxidized) and then electroplated with a thin layer of copper by reversing the current prior to removal of the parts from the bath. The clean, plated, polished, masked segments are then quickly transferred to a distilled water washing bath and then dried in an inert atmosphere. It may be necessary to remove the masking material after the plating process in order to avoid contamination of the bonding process. This decision will depend upon the specific masking material composition. The pattern plated segments are stored in a desiccated, inert atmosphere. The mating spacer/doubler disks are similarly prepared from a thicker (~2 to 10x) compatible material. The two sets of parts are transferred to an inert atmosphere glove box where they are interleaved. Figure III-3 outlines this assembly process.
The use of brush plating or "stamp pad" plating processes will involve effectively the same sequence of steps, the only difference relates to the method of providing the masking feature.
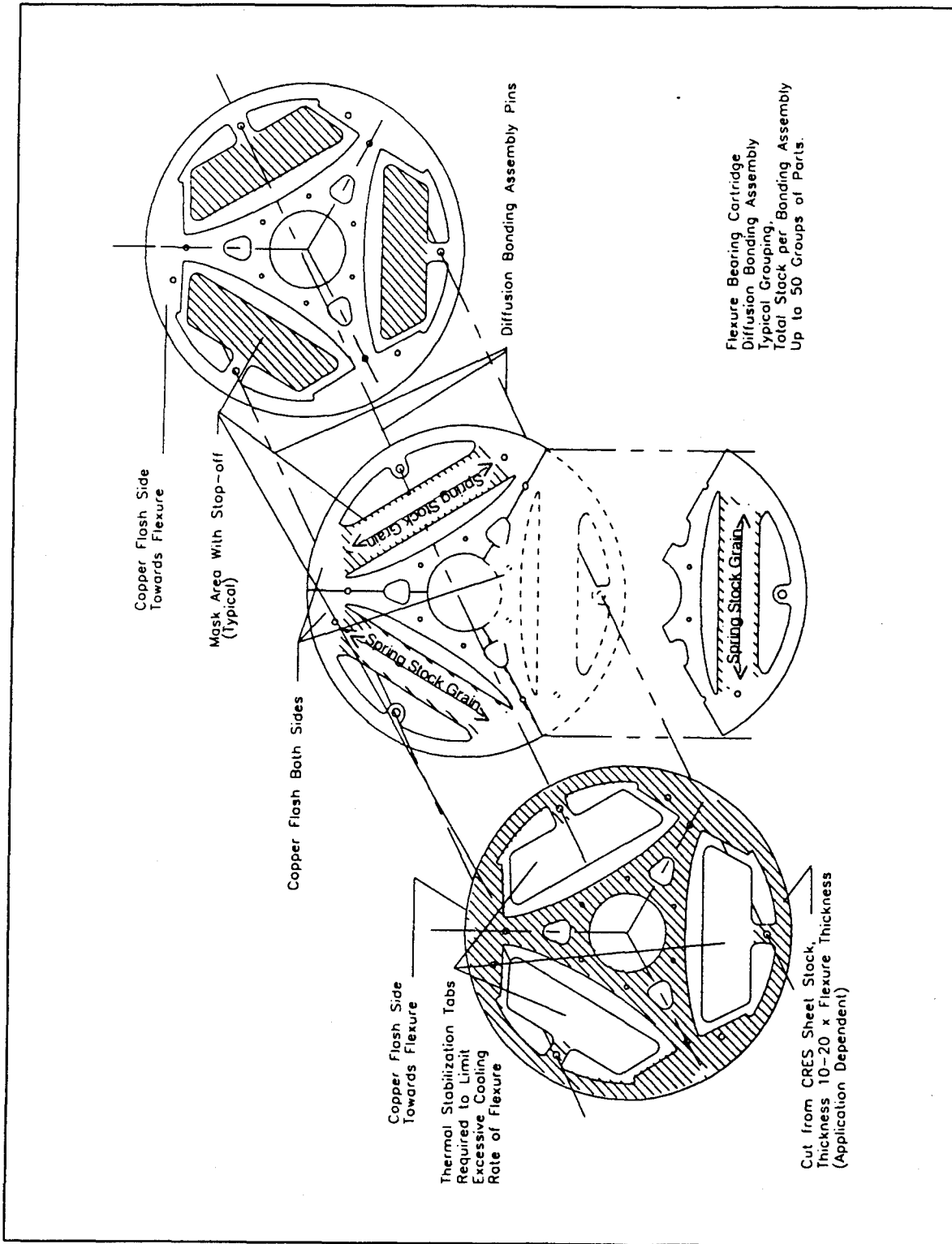
III-3; Flexure Bearing Diffusion Bonding Assembly

Approximately 50 such subassemblies are align stacked using assembly pins and mated with the diffusion bonding fixture. The fixtured assembly is placed in a gas-tight, ported cylindrical retort. The retort is designed with a metal bellows on one end so that the fixtured assembly can be axially loaded using an external press. The retort with its fixtured assembly is placed in a cylindrical muffle furnace, the ends of the retort being supported and loaded from the external press plungers. The retort inlet port is connected to a hydrogen gas source, and the retort exit port is vented through a catalytic exhaust vent. Prior to and during the bonding process, the void volume within the furnace, but external to the retort, is flushed with argon. During the same period, the retort volume is flushed with dry hydrogen. The furnace is heated until the fixtured assembly reaches the bonding temperature (~700 K), then the furnace is slowly cooled using dry nitrogen gas in place of the argon and hydrogen. Any copper oxide on the plated areas is readily reduced by the free hydrogen in the reducing atmosphere. The copper interfaces bond together, and the plated copper partially diffuses into the adjoining CRES, thus providing a solidly bonded copper joint.

The higher temperature CRES diffusion bonding process described in the proposal has been relegated to a backup process, with the copper diffusion bonded process becoming the baseline choice. This selection has been made because the copper bond exhibits more than adequate "infinite life" strength for this application, is more readily achieved, does not require subsequent tempering, and costs less than the CRES diffusion bonded interface. In Phase I it was discovered that in order to completely diffuse the copper into the parent CRES, and thereby achieve the diffusion bonded CRES joint, it is necessary to heat the parts up to the melting temperature of copper (1357 K)[10]. Uddeholm recommended that the bonding temperature be kept below 800 K to avoid the necessity for retempering the 716 CRES. It was also noted that the higher temperature processing tended to result in distorted parts unless the heat up/cool down were carefully controlled to minimize temperature gradients within the bonded assembly. Figure III-4 shows a cross section of the proposed Phase II furnace-retort-fixtured assembly.
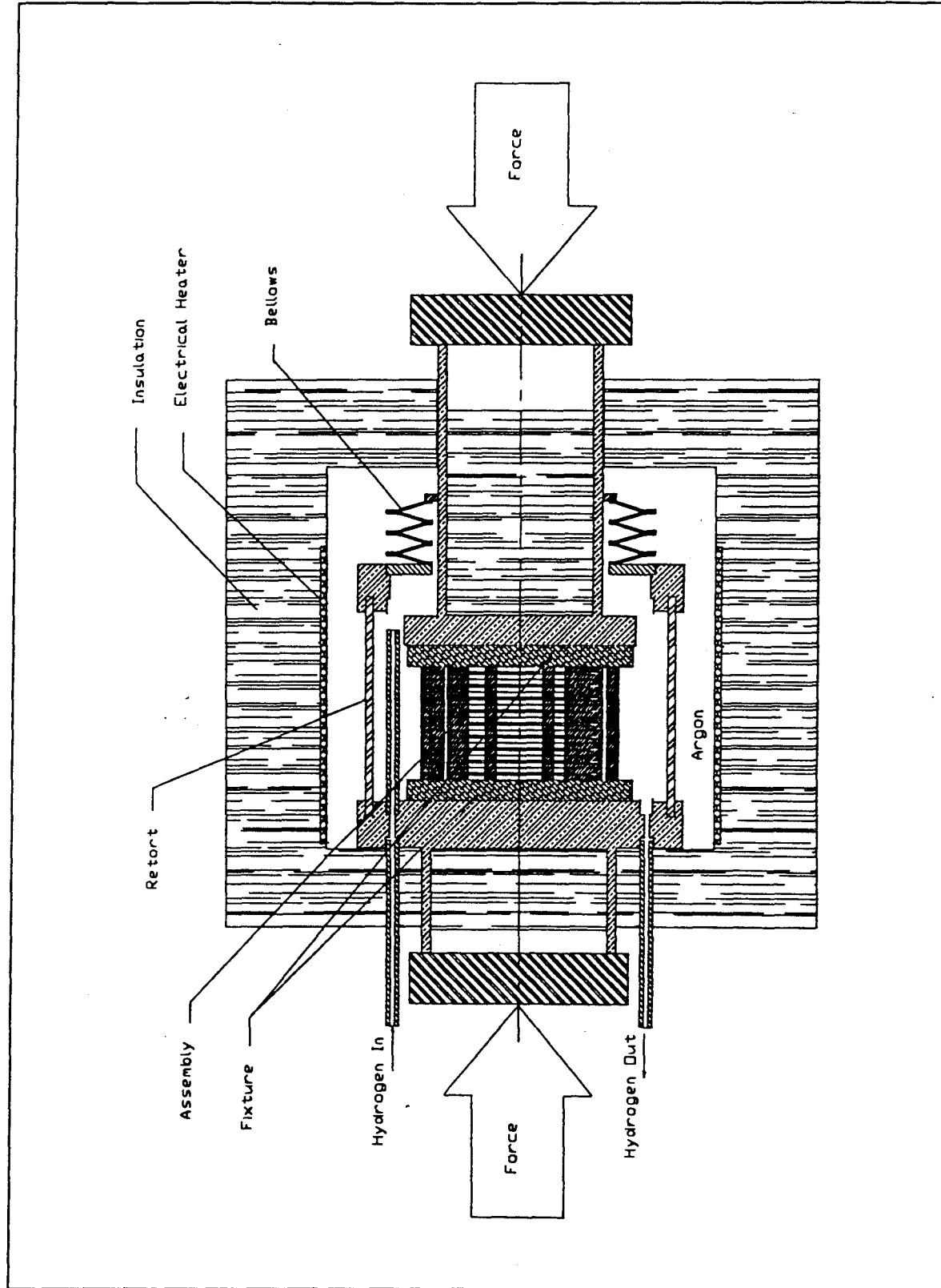
Figure III-4: Furnace-Retort-Fixtured Assembly Cross Section

The hydrogen atmosphere copper diffusion bonding process was selected over the fluxed brazing alternatives because it offers better "stack-up" dimensional control and it minimizes the risk of corroding, thus weakening, the flexure blades. Solder joints would not have adequate fatigue life. Adhesive bonded joints were excluded because they introduced complications in the subsequent machining and joining processes. The adhesives could also become a source of contamination to the thermodynamic cycle working fluid.

As part of the Phase II program, the bonding processes will be reexamined. The use of a small amount of titanium with the copper will be considered for both the copper and the CRES diffusion bonding process.

The basic diffusion bonded structure is shown in Figure III-5 prior to the final machining processes. If the goal is to fabricate a set of individual elements, the diffusion bonded assembly is first ground and honed on the OD and in the bore to create the close tolerance dimensions required by the bearings. Next, the center translating spider is EDM cut from the outer mounting rim and then the thermal stabilization tabs are EDM cut from the outer mounting rim.

If the goal is to fabricate an integrated bearing cartridge with metal rims such as shown in Figure III-6, the thermal stabilization tabs are EDM cut from the outer mounting rim, thus leaving the individual diffusion bonded elements with the central spider and the rim still attached. The desired quantity of elements are slipped within an appropriate length of tubing bored to line fit the OD and a similar smaller diameter tube is fit into the flexure element set ID. The edges of these tubes are rolled to mechanically retain the flexure elements. The resulting OD and ID rims are ground to dimension and then the central spider is EDM cut from the outer rim. Several precision grinding machines are available which can machine parts to the required accuracy.[11,12]

Section A-A

Difussion Bonded Flexure Module

2. Wire EDM cuts required to remove flexure thermal stabilization tabs, to seperate flexure cartridges, and to free center translating spider from outer mounting rim.(typ)

1. Grind/Hone ID and OD
to +/- 2 μ true round
and +/- 3 μ concentricity
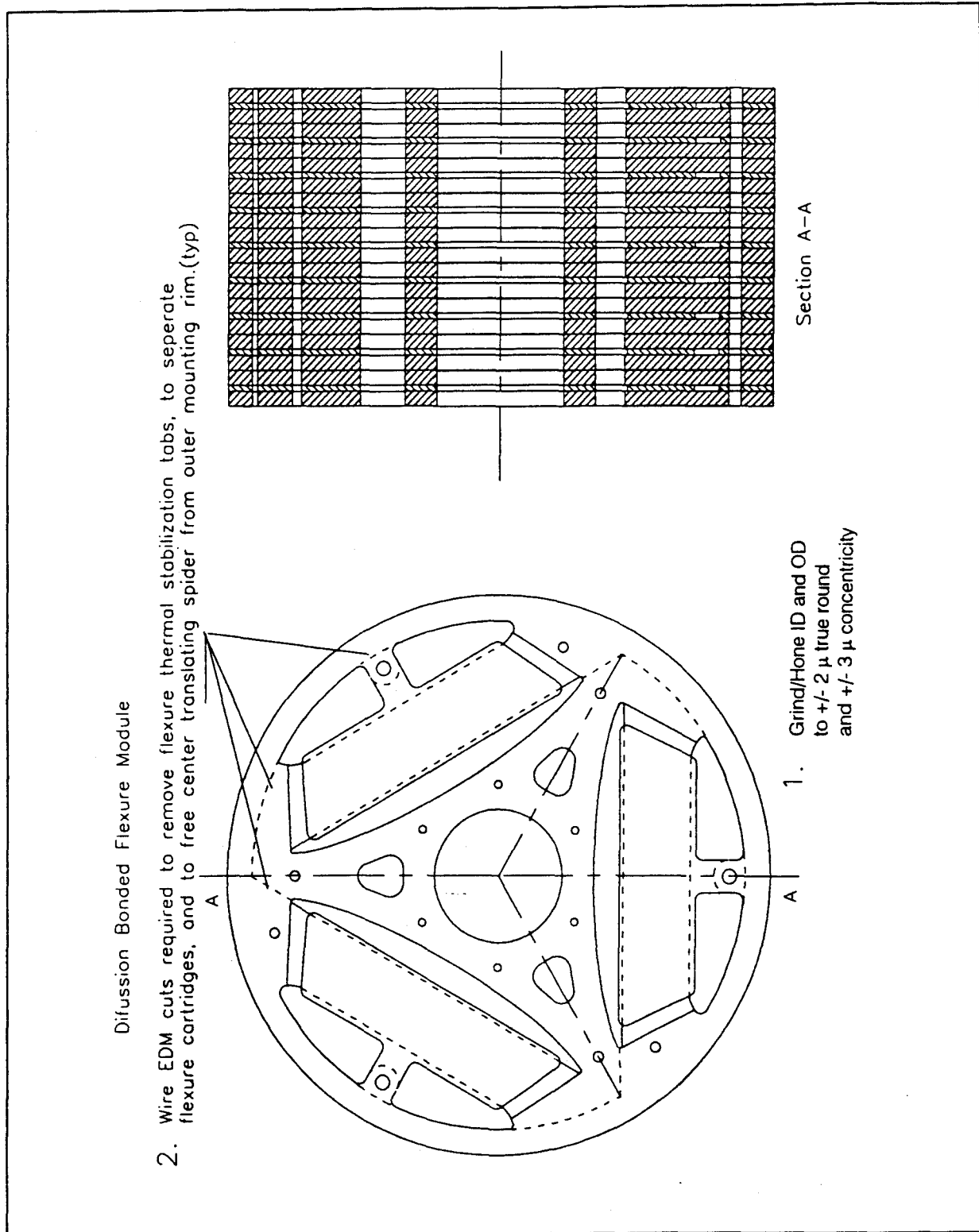
Figure III-5; Diffusion Bonded Flexure Module

The low bonding temperature allowed by the use of a copper joint could eliminate the need for "thermal stabilization tabs" to control the residual thermal stresses which could arise from rapid differential cooling during quenching. Elimination of the thermal stabilization tabs will reduce the machining steps outlined above. The elimination of the thermal stabilization tabs also will allow alternate assembly processes, such as the co-bonding of the flexures and the rims in one step. There are several different proven methods for forming the external and internal mechanical retaining rims, and several possible alternative materials. The two most obvious materials to be considered to match the thermal coefficient of expansion are stainless steel and zirconia.

The use of ceramic rims is particularly interesting because it will result in electrically isolating the flexure system from the mounting surfaces, thus allowing the flexure system to provide both the bearing and the power transfer functions. zirconia would currently be the ceramic of choice due to its thermal coefficient of expansion closely matching that of 716 CRES together with its inherent toughness. zirconia can be brazed to stainless steel with a silver, copper, indium, or titanium braze alloy at 1100 K. This might be an acceptable bonding temperature for the case where the stainless parts are diffusion welded together; however, assuming the use of a copper joint suggests that a lower temperature ceramic-CRES joint is required. To create these lower temperature joints, it is necessary to metallize the ceramic part surfaces to be joined. The metallized ceramic interface is then copper brazed to the copper-plated CRES surface. Figure III-6 shows one possible configuration of a precision linear flexure bearing cartridge with ceramic rims. This configuration is also identical to one using stamped CRES rims, or plasma sprayed ceramic rims, both of which are alternatives to be considered during the Phase II program.

Given a bonded, rimmed cartridge, the subsequent steps are to precision grind the OD and ID, followed by EDM machining of the cartridge to separate the spider from the rim.

Metallic Rim/
Frit Bonded
or
Ceramic Rim/
Braze Bonded

Lightening Hole/
Axial Access Port

A

Coil Mount/
Power Feed Pin Connection

Fixed Power Connection

Fixed Rigid Rim
(Insulated)

Flexure
Leaf

Translating
Hub Mount Holes

A

Translating
Rigid Spider

Translating
Rigid Rim
(Insulated)
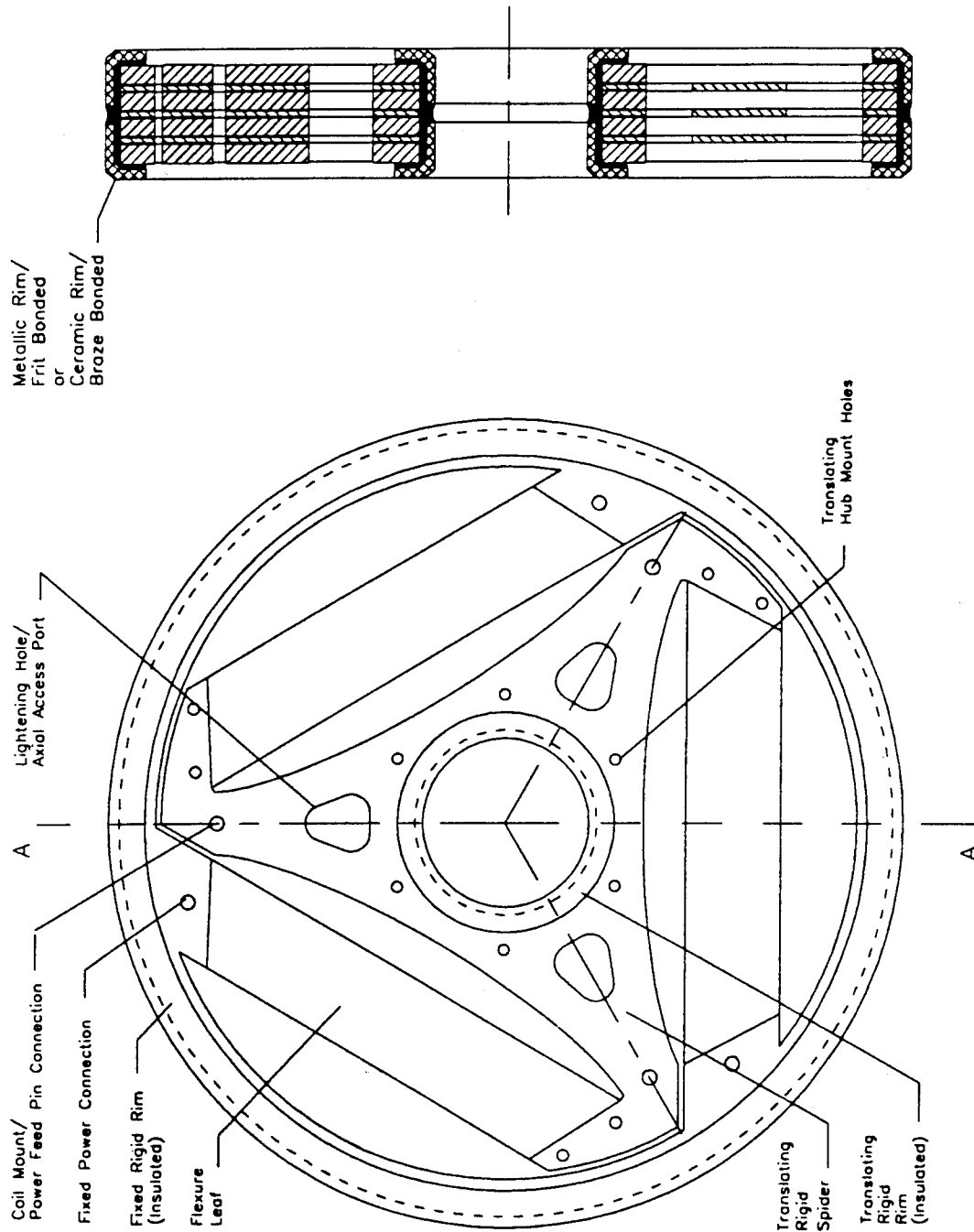
Figure III-6; Bonded Rim Precision Flexure Bearing Cartridge

## IV.0 BONDING STUDIES

### IV.1 Cleaning Techniques

Task 5B material selection for the flexure elements resulted in the selection of a Uddeholm Stainless 716 as the baseline material. The cleaning processes must therefore be applicable to martensitic stainless steels. For reasons of cost, manufacturability, and availability, the spacing elements used in the fabrication of the module could be ferritic or austenitic stainless steel, thus the cleaning process should be extendable to these materials. Because the parts are to be metallurgically bonded, it is important to assure that the bonding surface be suitably prepared during the cleaning process to be compatible with the bonding process. The tightly bonded oxide film that rapidly forms on a cleaned stainless steel surface is a hinderance to the bonding process. For this reason, the cleaning process shall be intimately associated with the plating process which involves the application of either a copper or nickel flash on the cleaned surfaces that are to be bonded. The surfaces should be initially treated in an alkaline cleaning bath, rinsed in de-ionized water, and then surface activated by cathodic treatment to remove any oxides.

### IV.2 Plating Techniques

It is necessary to provide either a copper or a nickel flash directly on the deoxidized freshly cleaned surfaces by anodic deposition without exposing the deoxidized surfaces to air. This can be most conveniently accomplished by using a bath which allows for both the cathodic and anodic processing by simply reversing the applied voltage. If the parts are to be diffusion bonded, the copper flash should be used. If the parts are to be bonded by brazing or soldering, the nickel flash would be appropriate.

Intrinsic to the fabrication process proposed for the linear flexure bearing module is the use of masked or pattern plating. Consideration of the costs associated with mask plating has resulted in the invention of the alternative process which is identified herein as "Wick Pad Pattern Plating." The process is based on the concept of brush plating but has been extended to incorporate the use of a wick pad that is continually saturated with the plating solution together with a special platen system that fixtures and couples the part to be pattern plated to the electrical plating power source. This process will be examined during Phase II.

Both brush plating and tank plating processes were experimentally confirmed as potentially suitable alternatives. The brush plating process was used to fabricate all the test parts. The brush plating process does not allow for the single bath - sequential cathodic-anodic treatment by voltage reversal technique. The following brush plating

process detailed below has successfully plated copper on 716 stainless steel (a 400 series type, no nickel, only chromium iron):

1. Wash parts in detergent
2. Rinse: All rinses are distilled water ($N_2$ sparged recommended)
3. Paper dry
4. Mask parts
5. Clean and deoxidize with BEC[1] 100;
     straight polarity, 10 V, 1.5 min. per side
     (both sides are cleaned even if only one side is to be plated)
6. Rinse
7. Etch with BEC 102;
     reverse polarity, 13 V, 2.5 min. per side plated
     If both sides are to be plated, work both sides simultaneously - 5 min. total.
8. Rinse
9. Desmutt with BEC 103;
     reverse polarity, 13 V, 1.5 min. per side
10. Rinse
11. Activate with BEC 102;
     straight polarity, 12 V, 1.5 min. per side
12 Rinse
13 Plate with BEC 335 (soft copper, acid type);
     straight polarity, 9 V, 2.5 min. per side
14. Rinse
15. Paper dry
16. Store in inert atmosphere (dry nitrogen, argon, etc)

---

[1]BEC refers to brush plating solutions from Brooktronics Engineering Corporation, North Hollywood, California[13].

IV.3 Soldering Techniques

Stainless steels can be soldered by several different processes:

- In an ambient gaseous environment using specially prepared soldering pastes which incorporate both the deoxidizing flux and the solder alloys.

- In a hot oil bath using flash-plated stainless parts and solder alloy foil.

- In a hot oil bath using flash-plated stainless parts and plated solder alloy.

Consideration of these possible methods together with an evaluation of the properties of the various solder alloys, concludes that the third process (using 95% Tin - 5% Lead) solder would be appropriate. The bath temperature for this process is about 250°C. The maximum obtainable shear strength at 20°C is 43 MPa. Since the fatigue life of soldered joints is so low, it would be necessary to incorporate either mechanical fastening or microspot in the cyclically stressed regions. Due to this added complexity, this method of bonding was not examined in further detail during Phase I. It will be reconsidered in Phase II.

IV.4 Brazing Techniques

Stainless steels can be brazed by several different processes:

- In an ambient gaseous environment using specially prepared brazing pastes which incorporate both the deoxidizing flux and the brazing alloys.

- In a vacuum or reducing gaseous environment using flash-plated stainless parts and brazing alloy foil.

- In a vacuum or reducing gaseous environment using flash-plated stainless parts and plated brazing alloy.

Consideration of these possible methods, together with an evaluation of the properties of the various brazing alloys has concluded that using a silver based brazing alloy could be an appropriate process. The furnace temperature for this process depends on the specific alloy and ranges from 620°C to 870°C. The maximum obtainable shear strengths at 20°C range from 170 to 310 MPa. Since these processing temperatures exceed those required to diffusion bond copper to copper, and since the shear strengths are approximately the same as the copper-copper joint, there is no apparent reason to use brazing techniques rather than plated metal diffusion bonding. (Actually,

the processes are quite similar, the difference being that the diffusion process operates in the solid state whereas the brazing process requires liquification of the brazing alloys.)

IV.5 Diffusion Bonding Techniques

Stainless steel can be diffusion bonded by using flash-plated parts in a vacuum or in a reducing gaseous environment. The furnace temperature for this process is dependent on the fixture pressure and the time at temperature; however, the prevalent process requires about 0.5 MPa and a few minutes time at a temperature equal to or greater than the melting temperature of copper (~1357 K). The maximum obtainable shear strength is that of the parent metal.

Copper can be diffusion bonded to copper in a vacuum or in a reducing gaseous environment. The furnace temperature for this process is dependent on the fixture-induced interface pressures and the time at temperature. In Phase I copper-plated 716 stainless steel was successfully diffusion bonded to copper-plated 716 stainless steel using 30 MPa contact pressure, in either a vacuum or in a reducing gaseous environment (hydrogen) held at ~750 K for 1 hr.

The infinite cycle fatigue strength (actually a maximum strain) for the copper joint is adequate for the flexure design. The lower processing temperature eliminates any potential problems with the tempering of the 716 stainless steel. Thus the copper-copper diffusion joint was selected for the Phase I fatigue strength studies. It is possible that an advantage could be obtained by using either a 40% copper-60% silver plating or a 65% tin-35% nickel plating as the solid-solid self-diffusing interface material. The diffusion bonding temperatures for these intermetallic compounds should be less than that required by the copper-copper process, and the shear strength could be higher. Such alternatives will be examined in Phase II.

IV.6 Wire EDM Implications

Intrinsic to the design proposed for the precision linear flexure bearing module is the concept of fabricating the module so that the inner and outer bearing surfaces are structurally interconnected during the final machining process so as to keep any machining forces from deforming the flexure members. This requires that there be a nonstressful separation process to free the inner and outer surfaces after the final machining. EDM is the appropriate process, given the narrow kerf required after this separation. Because of the difference in physical and electrical properties of the flexure materials and the bonding agents, it is important that any potential problems with EDM

cutting of these sandwiched structures be identified and used as part of the selection process.

Not listed in the candidate bonding techniques is adhesive bonding. This process was rejected since it was assumed that the dielectric bonding material (epoxy, etc.) layers would interfere with or stop the EDM machine process. This assumption should be verified. If there are no difficulties with EDM processing of adhesive bonded systems, their use should be considered and the appropriate processes and controls documented.

IV.7  Mechanical Fastening

The use of rivets to aid in the assembly and to resist the shearing stress in units fabricated by either soldering or adhesive bonding is considered necessary. The use of hollow copper rivets will probably be required in the brazed or diffusion bonded designs also, not for structural reasons but for installation reasons. Since the flexures could also act as electrical conductors to provide power to the motor coil, the use of hollow copper rivets would serve to aid in such an application.

IV.8  Spot Welding

Consideration should be given to microspot welding as a method to assure that the shear loads are transmitted from the flexures to the doublers. This alternative will also be examined in Phase II.

IV.9  Diffusion Bonding Experiment

Figure IV-1 details the diffusion bonding test coupons, both in dimension and in bonding aid preparation and location.

| Dash # | Surface A | Surface B | Surface C | Surface D |
|--------|-----------|-----------|-----------|-----------|
| -1 | untreated | untreated | untreated | untreated |
| -2 | cu plated | untreated | untreated | untreated |
| -3 | cu plated | untreated | cu plated | untreated |
| -4 | cu plated | cu plated | untreated | untreated |
| -5 | cu plated | cu plated | cu plated | cu plated |

Material, 0.0100, Uddeholm 716 CRES

Dimensions, 0.000 = +/- 0.0025
0.0000 = +/- 0.0001
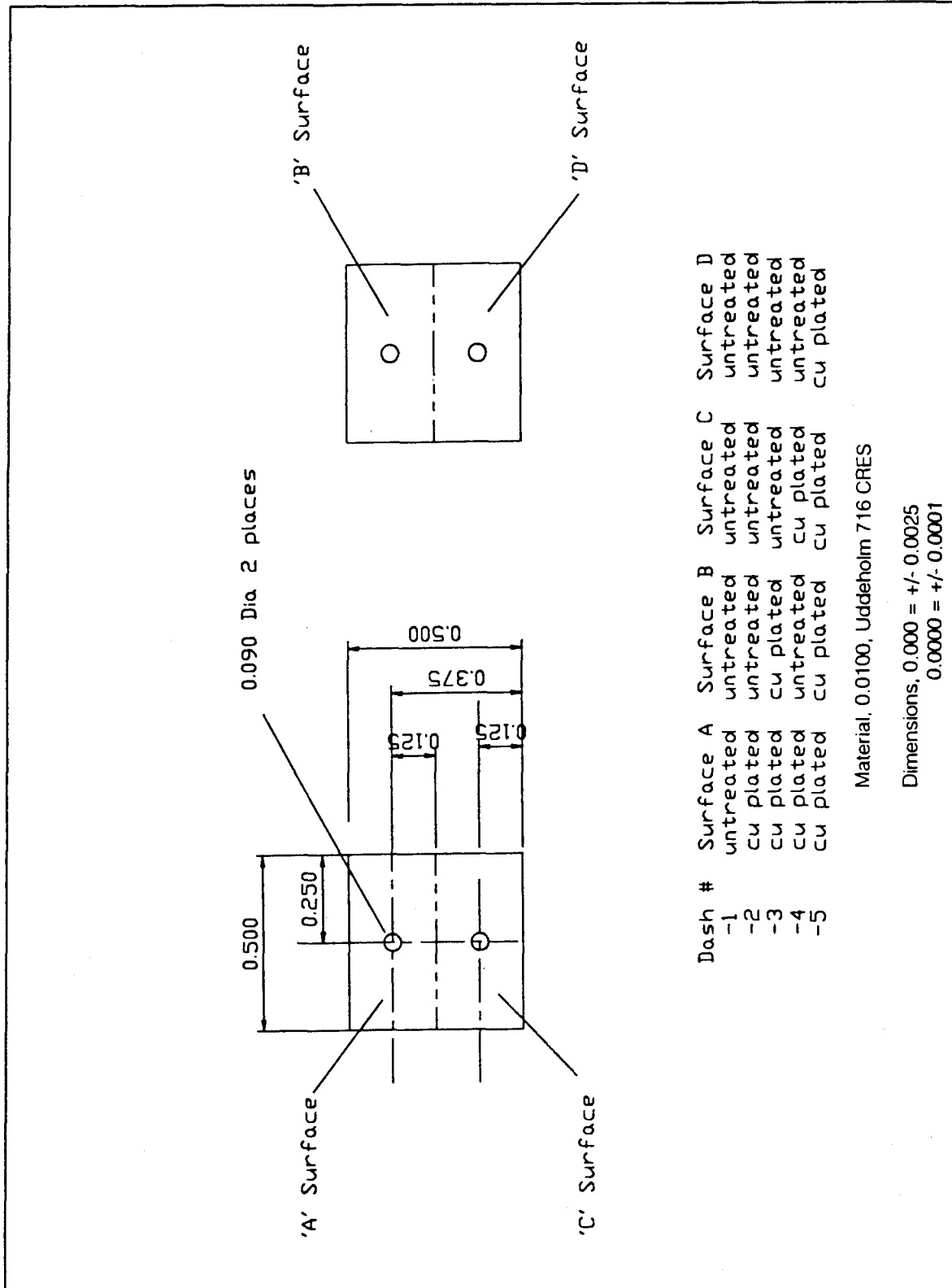
Figure IV-1; Diffusion Bonding Test Coupon

# PRECISION LINEAR FLEXURE BEARING CARTRIDGE
### PHASE I FINAL REPORT

Figure IV-2 shows a typical diffusion bonding coupon test stack, which is composed of 47 coupons arranged in the following sequence:

```
                A    -1    C
                B          D
                B    -4    D
                A          C
C   -3          A          A    -3    C
D               B          B          D
                A    -4    C
                B          D
B   -4          D          B    -4    D
A               C          A          C
                A    -5    C
                B          D
A   -4          C          A    -4    C
B               D          B          D
                B    -6    D
                A          C
C   -7          A          A    -3    C
D               B          B          D
                A    -6    C
                B          D
D   -2          B          B    -4    D
C               A          A          C
                A    -1    C
                B          D
A   -6          C          A    -6    C
B               D          B          D
                B    -4    D
                A          C
A   -7          C          A    -7    C
B               D          B          D
                A    -5    C
                B          D
```

This sequence was repeated and a final -1 part was added to assure release from the fixture.  After the parts were bonded, the peel and shear properties were evaluated. Only the copper-plated to copper-plated surfaces proved to be acceptable. Photomicrographs of the copper-copper interface were obtained, (Figures IV-3 through IV-5). It is apparent from these results that 1 hr at 730 K in a hydrogen furnace produces an acceptable bond. It is possible that the failure shown for the part processed at 670 K was due to an improperly deoxidized surface prior to the copper plating.
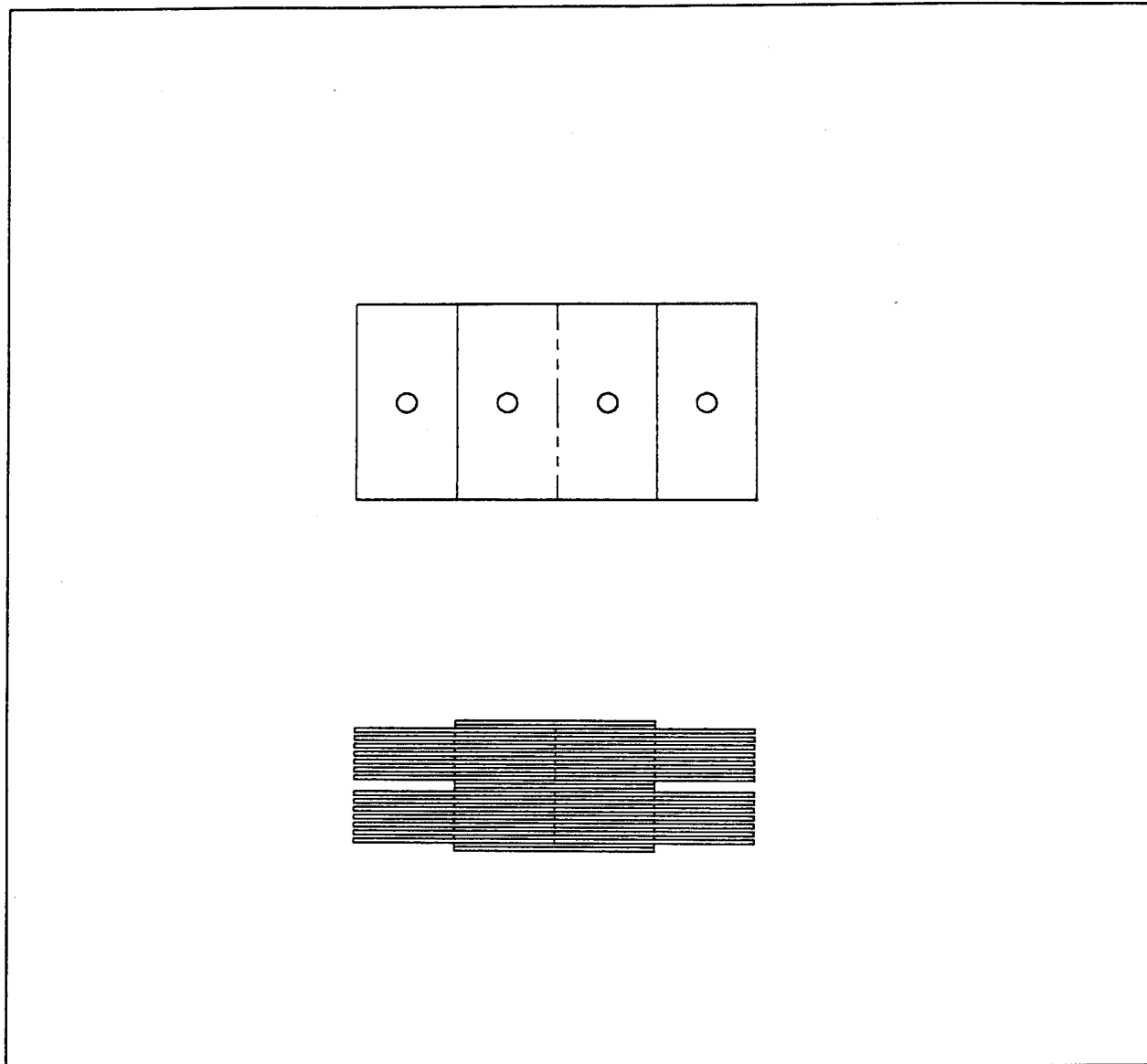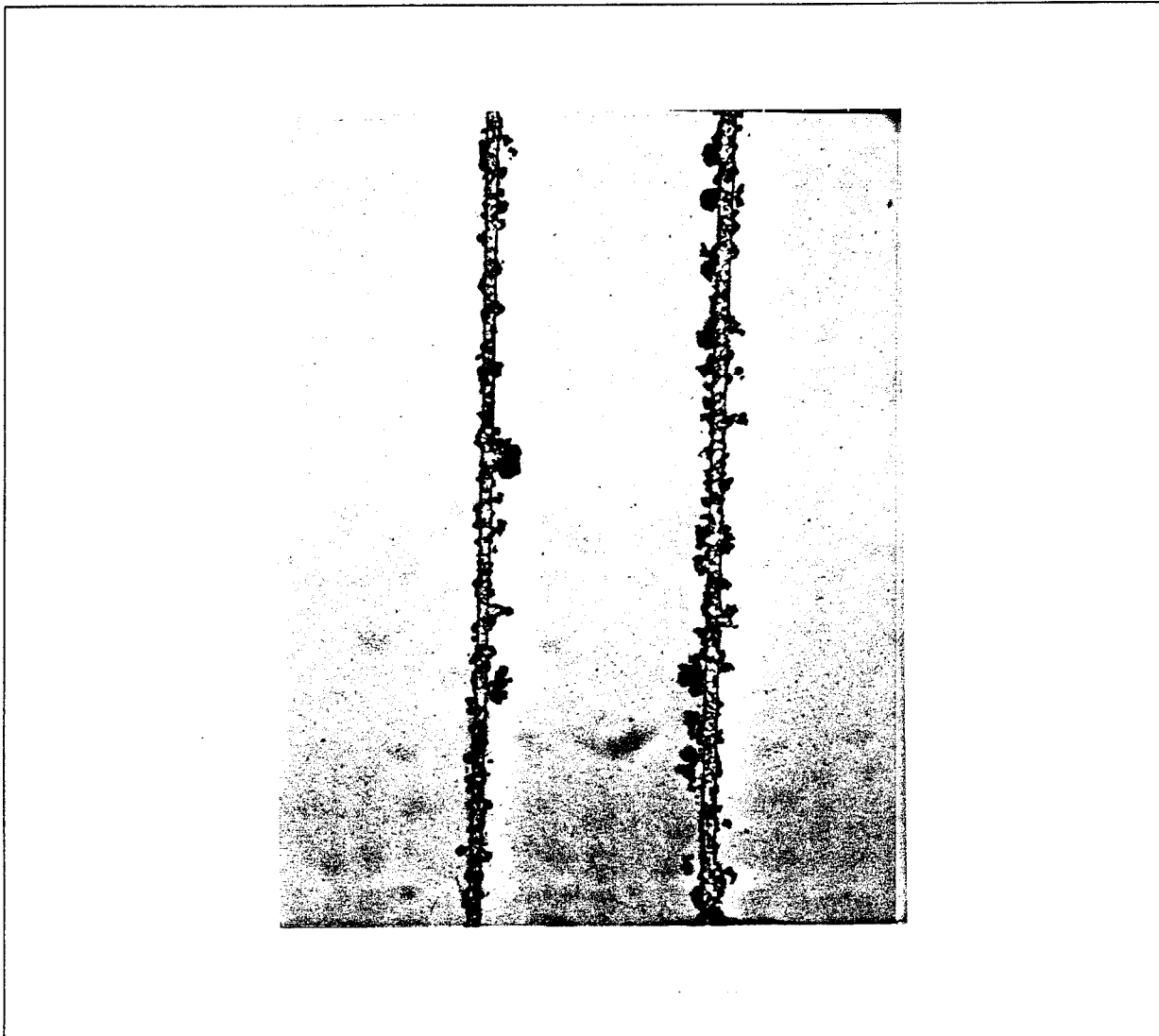
Figure IV-2; Diffusion Bonding Coupon Stack
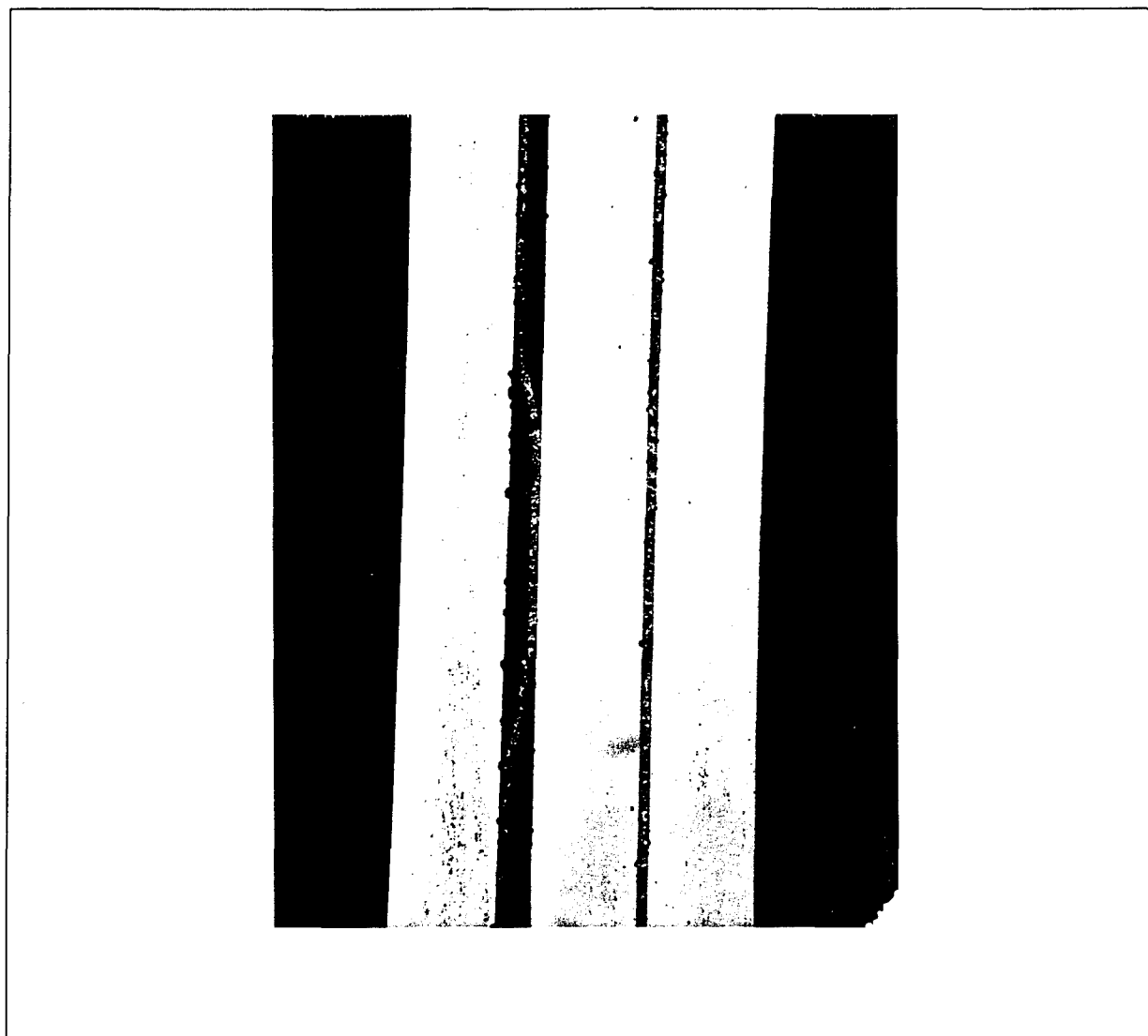
Figure IV-3; Photomicrograph of Diffusion Bonded Test Coupon: 1 hr, 670 K, 35 Mpa - 110x

Figure IV-3 shows separation between 716 stainless steel and copper on both sides of one interface. The copper-copper interface has completely diffused. The separation may have been due to improper surface preparation prior to the copper plating.
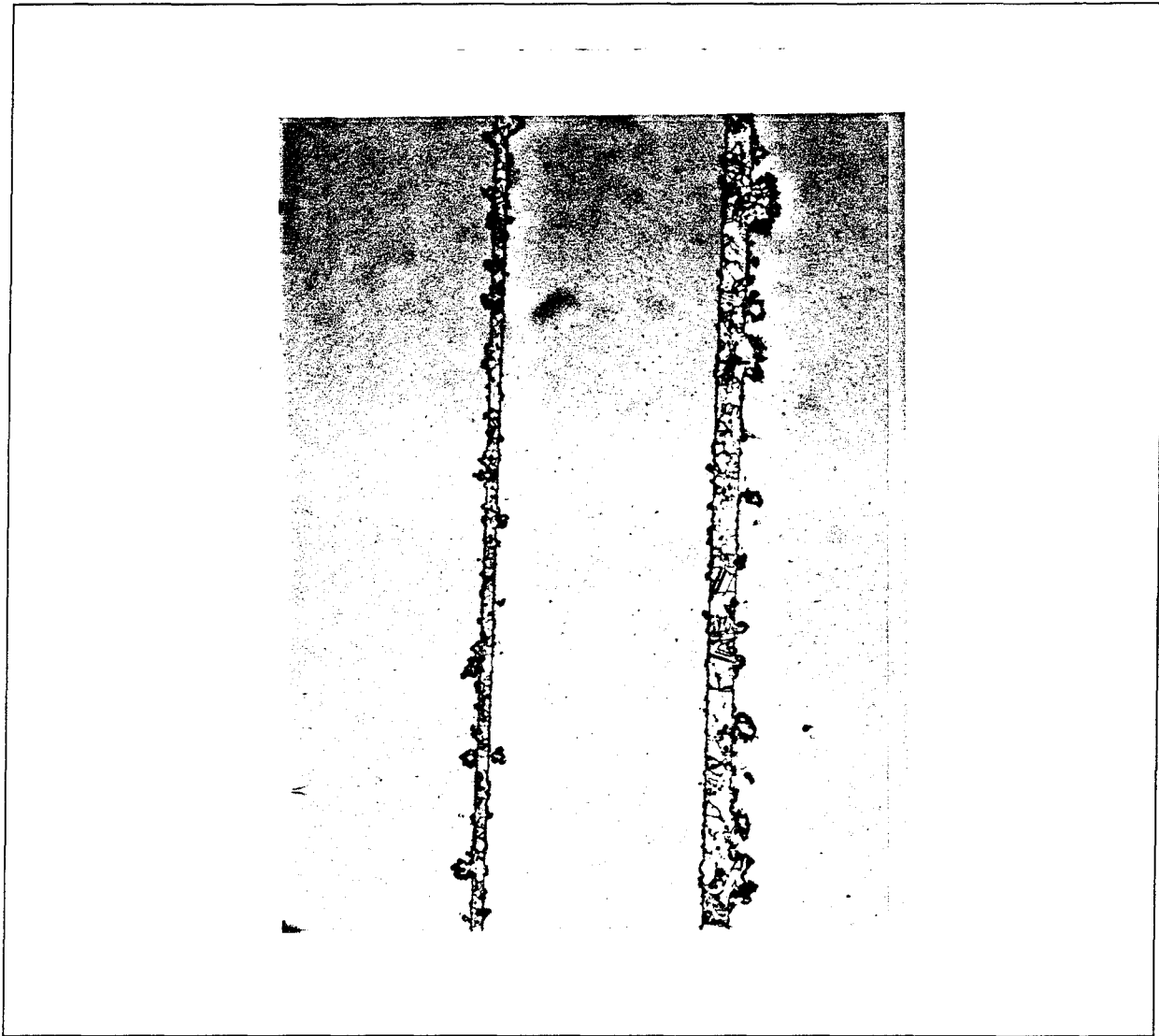
Figure IV-4; Photomicrograph of Diffusion Bonded Test Coupon: 4 hrs, 730 K, 35 Mpa - 220x

Figure IV-4 shows complete bonding between 716 stainless steel and copper on both sides of one interface. The copper-copper interface has completely diffused and migration into the 716 stainless steel has apparently occured.

Figure IV-5; Photomicrograph of Diffusion Bonded Test Coupon: 1 hr 730 K, 35 Mpa - 220x

Figure IV-5 shows complete bonding between 716 stainless steel and copper on both sides of one interface. The copper-copper interface has completely diffused and migration into the 716 stainless steel has apparently occured.

## V.0 FATIGUE TESTING STUDIES

### V.1 Fatigue Testing Machine Considerations

In order to derive the S-N of cycles to failure probability diagram, it will be necessary to run between $10^6$ and $10^7$ cycles in a reasonable amount of time. For the purposes of establishing the cycle rate, assume that each set of the data is to be obtained within a 5 day run. The drive frequency would then be between 25 and 250 cps.

Fatigue testing machines based on the voice coil motor drive design are usually limited to 100 g's maximum acceleration. Since the displacement equation is of the form

$$\delta(t) = \delta_0 \sin \omega t$$

$\delta_0$ = Maximum Deflection    $\omega$ = Frequency    $t$ = Time

the acceleration relationship is obviously

$$a = \frac{d^2 \delta_0 \sin \omega t}{d^2 t} = -\delta_0 \omega^2 \sin \omega t$$

thus,

$$\delta_0 \omega^2 = \delta_0 (2\pi f)^2 \leq 98066.5 \frac{cm}{sec^2}$$

$$f = \frac{\omega}{2\pi}$$

Therefore, corresponding to 25 cps < f < 250 cps;

$$4\,cm < \delta_0 < 0.04\,cm$$

The lower frequency places no design constraint on the test specimen design; the upper frequency does however. This limitation on the upper drive frequency can be circumvented if the test specimen is configured as a resonant part. As a compromise, to maximize the options available, the test specimen will be designed as a resonant part with a natural frequency of ~250 cps, but with a maximum displacement of ~0.25 cm.

### V.2 Resonant Flexure Analysis

Assume that the fatigue test specimen is a thin rectangular beam with one built-in end and the other end constrained to move sinusoidally between the deflection limits with the beam end slope being maintained level (dy/dx = 0 @ x = L). The natural frequency of such a system is dependent on the material properties of the beam, its geometry, and the mass attached to the free end. As a first approximation, Rayleigh's method is adequate:

Potential Energy at Maximum Deflection = Kinetic Energy at Neutral Position

which can be expressed mathematically as

$$\frac{1}{2}\int_0^L EI\left(\frac{d^2y}{dx^2}\right)^2 dx = \frac{1}{2}\int_0^L \mu\omega^2 y^2 dx + \frac{1}{2}M\omega^2\delta_0^2$$

$E$ = Material modulus of elasticity   $I$ = Section modulus of elasticity
$M$ = Mass Vibrating   $\mu$ = Weight per unit length

For a beam of constant cross section, the relationship reduces

$$\omega^2 = \frac{EI\int_0^L \left(\frac{d^2y}{dx^2}\right)^2 dx}{M\delta_0^2 + \mu\int_0^L y^2 dx}$$

To match the boundary conditions, the assumed shape for the vibrating beam is

$$y = \frac{\delta_0}{2}\left(1-\cos\frac{\pi x}{L}\right)$$

from which

$$\frac{d^2y}{dx^2} = \frac{\delta_0}{2}\left(\frac{\pi}{L}\right)^2 \cos\frac{\pi x}{L}$$

Solving the integral equation, the result is

$$\omega^2 = \frac{\left(\frac{Eg}{\rho}\right)\left(\frac{h}{L^2}\right)^2 \frac{\pi^4}{12}}{\left(3 + 8\frac{M}{m}\right)}$$

$\rho$ = Density   $g$ = Gravitation constant
$M$ = Mass of beam   $m$ = Distributed mass applied at the end of the beam

Solving for the beam length, the result is

$$L = \frac{1}{2}\sqrt{\frac{\pi h}{f}\sqrt{\frac{\left(\frac{Eg}{\rho}\right)}{9 + 24\frac{M}{m}}}}$$

$h$ = Height

For steel,
$$\sqrt{\frac{Eg}{\rho}} = 496,635\frac{cm}{sec}$$

Thus assuming a thickness, h, equal to 0.025 cm. and the end mass, M, approximately twice the flexure mass, m, the following results are obtained:

$$f = 25 \text{ cps, } L = 7.19 \text{ cm}$$
$$f = 250 \text{ cps, } L = 2.27 \text{ cm}$$

## V.3 Bending Beam Stress Analysis/Fatigue Testing Machine

To complete the design analysis it is necessary to examine the stress-deflection relationship for the fatigue test beam subjected to the end conditions assumed in the vibration response analysis. Figure V-1 shows the beam deflection shape when subjected to the static and dynamic loading imposed by the assumed end conditions.

For such a beam, linear analysis will result in the following solution:

$$\delta_0 = -\frac{PL^3}{12EI} = -\frac{M_1L^2}{6EI}$$
$$P = \text{Force}$$
$$M_1 = \text{Moment}$$

The maximum stress occurs at the outer fiber next to the ends. The linear analysis definition is

$$\sigma_{max} = \text{Maximum stress}$$
$$\sigma_{max} = \frac{M_1 h}{2I}$$

Thus,

$$\delta_0 = \left(\frac{\sigma_{max}}{3E}\right)\left(\frac{L^2}{h}\right)$$

Simultaneous solution with the results obtained above gives

$$\delta_0 = \frac{\pi}{12f}\left(\frac{\sigma_{max}}{E}\right)\frac{\sqrt{\frac{Eg}{\rho}}}{\sqrt{9 + 24\frac{M}{m}}}$$
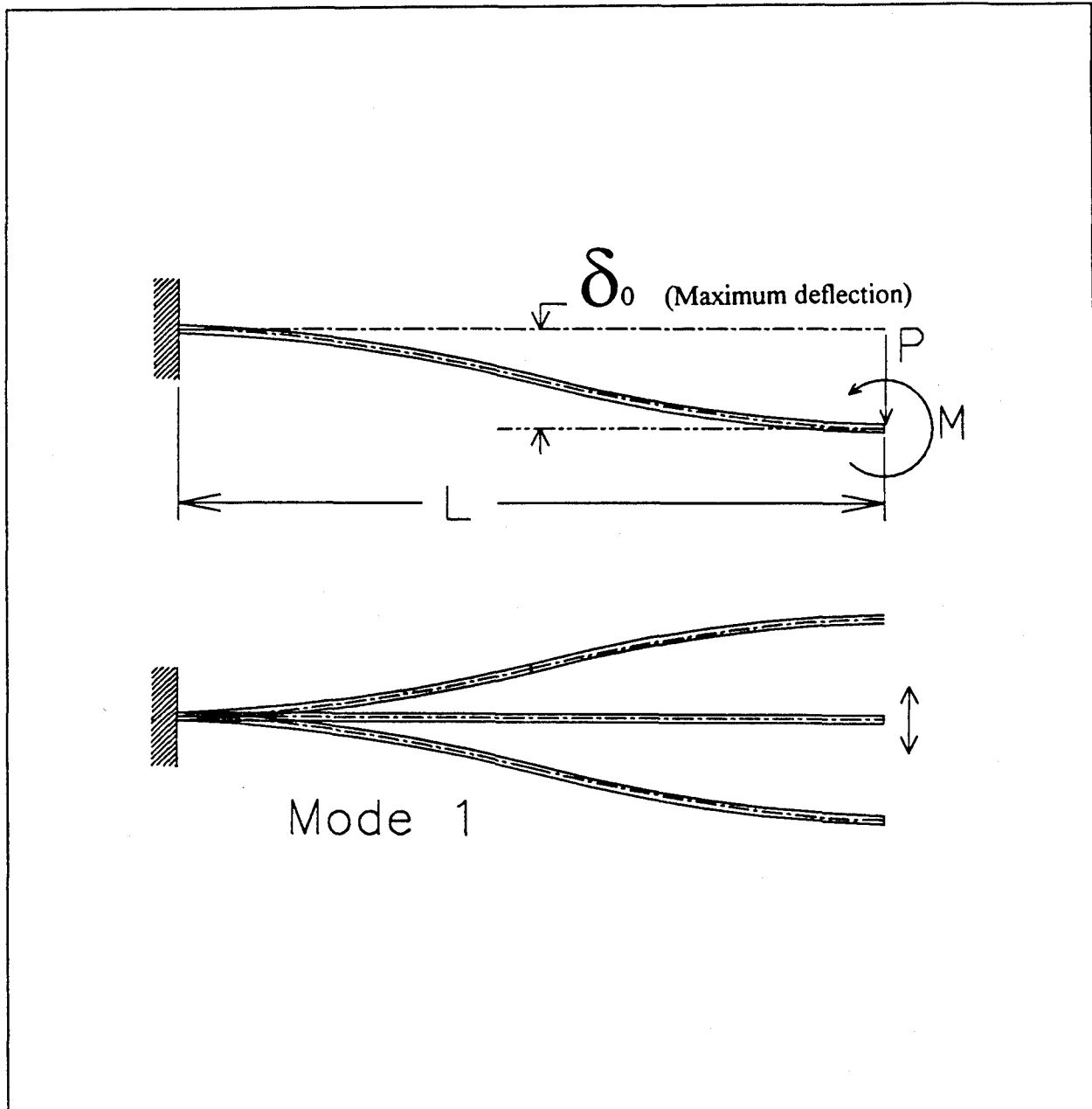
Figure V-1; Cantilever Beam with Free End Slope = 0

For the Uddeholm 716 stainless steel strip:

> Young's modulus = 220,000 Mpa
> Ultimate tensile strength = 1810 Mpa
> Reverse bending fatigue limit ratio = 0.41 (50% probability of failure)

Assuming a drive frequency of 250 cps and a mass ratio (M/m) of 2,

$$\delta_0 = 0.232 \text{ cm}$$

Thus a beam thickness, h, of 0.025 cm, a beam length, L, of 2.5 cm, a drive frequency, f, of 250 cps, a mass ratio, M/m of 2, and a deflection of 0.25 cm appear appropriate. For the actual fatigue testing, it was more convenient to effectively double the length of the beam, constrain the beam ends to maintain the slope and displacement equal to zero, and cyclically displace the center of the beam. Figure V-2 depicts this configuration.

The problem with this approach is that the electromagnetic driver would be operating at about 600 g, which is almost an order of magnitude greater than commercial hardware design capacity. To circumvent this difficulty, a fatigue tester based on the principles of the Frahm "dynamic vibration absorber" was developed [14,15]. Figure V-3 is a mechanical schematic of the Frahm dynamic vibration absorber.
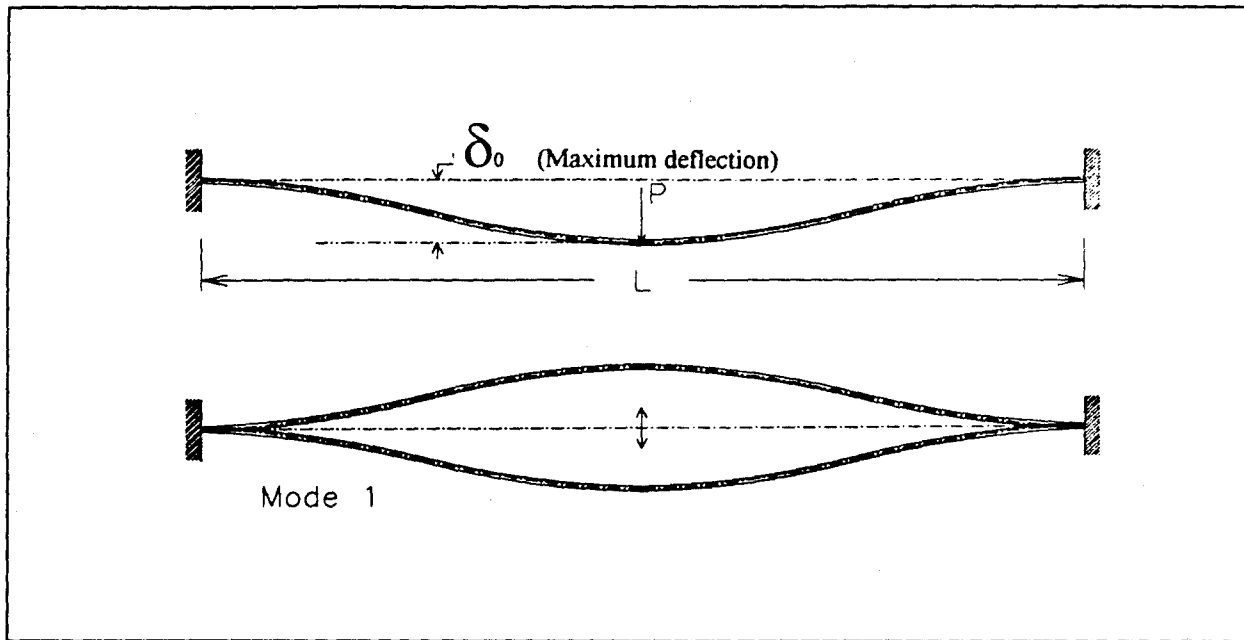
Figure V-2; Dual Cantilever, Cyclically Displaced Center, Beam Fatigue Testing Schematic
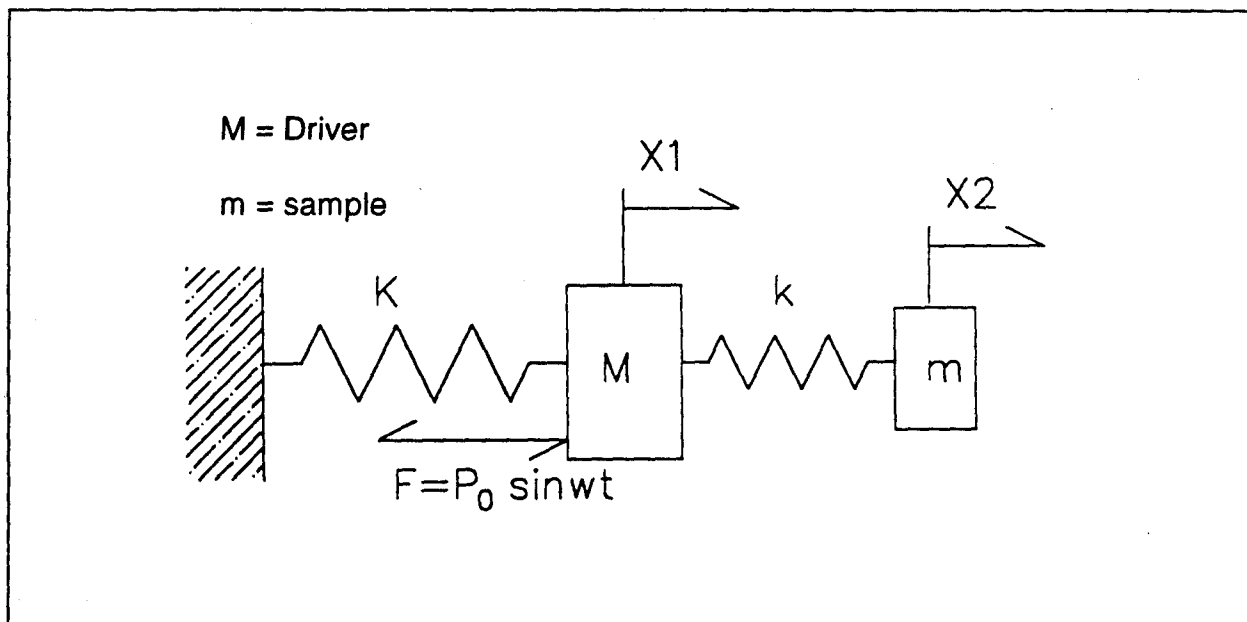


Figure V-3; Frahm Dynamic Vibration Absorber Schematic

The equations of motion for the Frahm dynamic vibration absorber can be written as

$$M\frac{d x_1^2}{dt^2} + (K+k)x_1 - kx_2 = P_0\sin\omega t$$

$$m\frac{d x_2^2}{dt^2} + k(x_2 - x_1) = 0$$

$x_1$ = Displacement of M from neutral  $x_2$ = Displacement of m from neutral

By defining:

$$\omega_n = \left(\frac{k}{m}\right)^{0.5} - \text{the natural frequency of the absorber}$$

$$\Omega_N = \left(\frac{K}{M}\right)^{0.5} - \text{the natural frequency of the machine}$$

$$P_0 = \text{peak drive force}$$
$$\omega = \text{the drive frequency}$$

$K$ = Spring constant
$k$ = Spring constant between $M$ and $m$

the solution to the equations of motion becomes

$$x_1 = \frac{P_0}{K}\frac{\left(1-\frac{\omega^2}{\omega_n^2}\right)}{\left(1-\frac{\omega^2}{\omega_n^2}\right)\left(1+\frac{k}{K}-\frac{\omega^2}{\Omega_N^2}\right)-\frac{k}{K}}\sin\omega t$$

$$x_2 = \frac{P_0}{K}\frac{1}{\left(1-\frac{\omega^2}{\omega_n^2}\right)\left(1+\frac{k}{K}-\frac{\omega^2}{\Omega_N^2}\right)-\frac{k}{K}}\sin\omega t$$

Thus, as

$\omega \rightarrow \omega_n$
$x_{1\ peak} \rightarrow 0$
$x_{2\ peak} \rightarrow P_0/k$

The absorber mass will undergo large excursions, but the driver will hardly move. This will solve the problem of excessive forces being required by the driver; in fact, a piezoelectric driver could be used rather than an electromagnetic voice coil driver.

To resolve difficulties with the actual geometry, the flexure fatigue coupons will be mounted in pairs, the connection to the main mass being through off-set yokes and stiff flexures mounted parallel to the drive direction to allow longitudinal movement of the flexures and to eliminate any extra moments about the flexure built-in ends. The motion of the central area of the flexures will be measured referenced to the main mass; however, because the main mass is effectively motionless, the deflection of the beams could also be measured from the reference ground. Figure V-4 is a mechanical schematic of the total concept, and Figure V-5 is a photograph of the actual hardware.
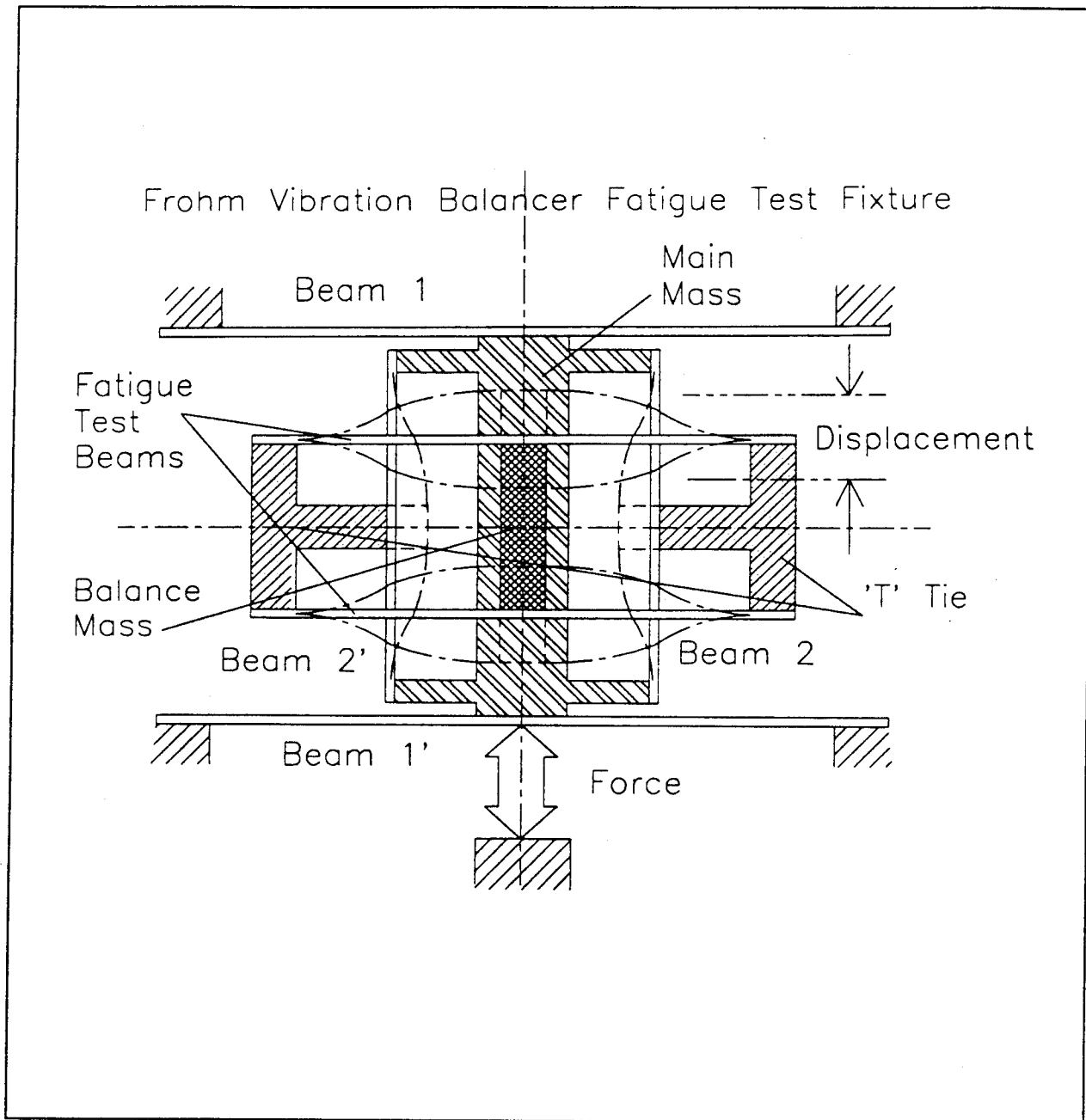
Figure V-4; Frahm Dynamic Vibration Balancer Fatigue Testing Machine
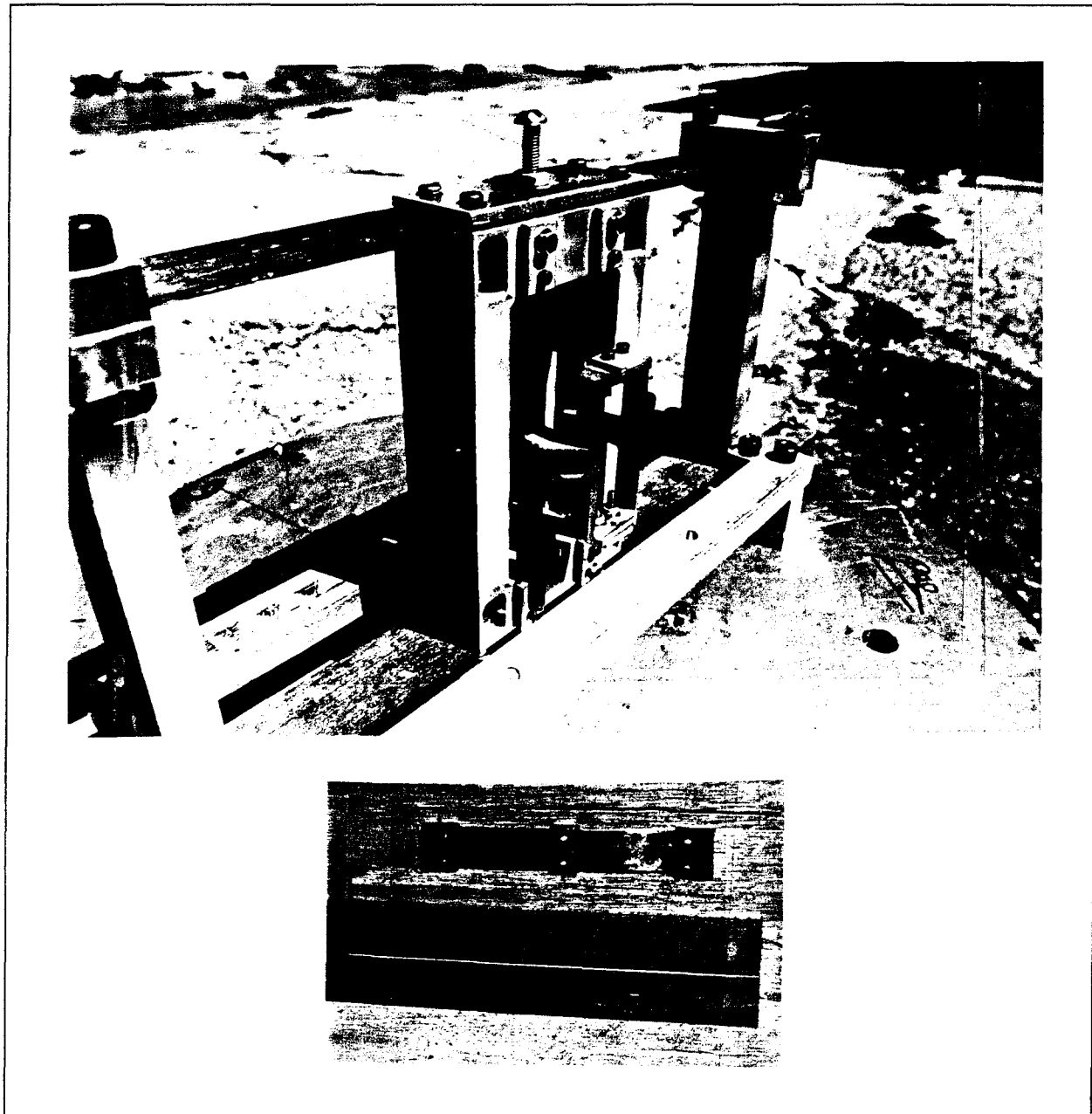
Figure V-5; Frahm Dynamic Vibration Balancer Fatigue Testing Machine and a sample part.

## V.4 Test Specimen Flexure Design

Based on the analysis presented, the flexure test specimen design will be fabricated as shown in Figure V-6. Figure V-7 shows the assembly layout from which the test specimens are cut using EDM to eliminate edge stresses. Figure V-8 shows the details used to fabricate the diffusion bonded assembly.

Fatigue test beams were fabricated with unpolished edges, with chemically polished edges, and with mechanically polished (Harperized) edges so that the effect of edge finish could be evaluated. Figure V-9 shows photomicrographs of typical unpolished (photochemically etched) edges, Figure V-10 shows photo-micrographs of typical chemically polished edges, and Figure V-11 shows photomicrographs of mechanically polished edges.
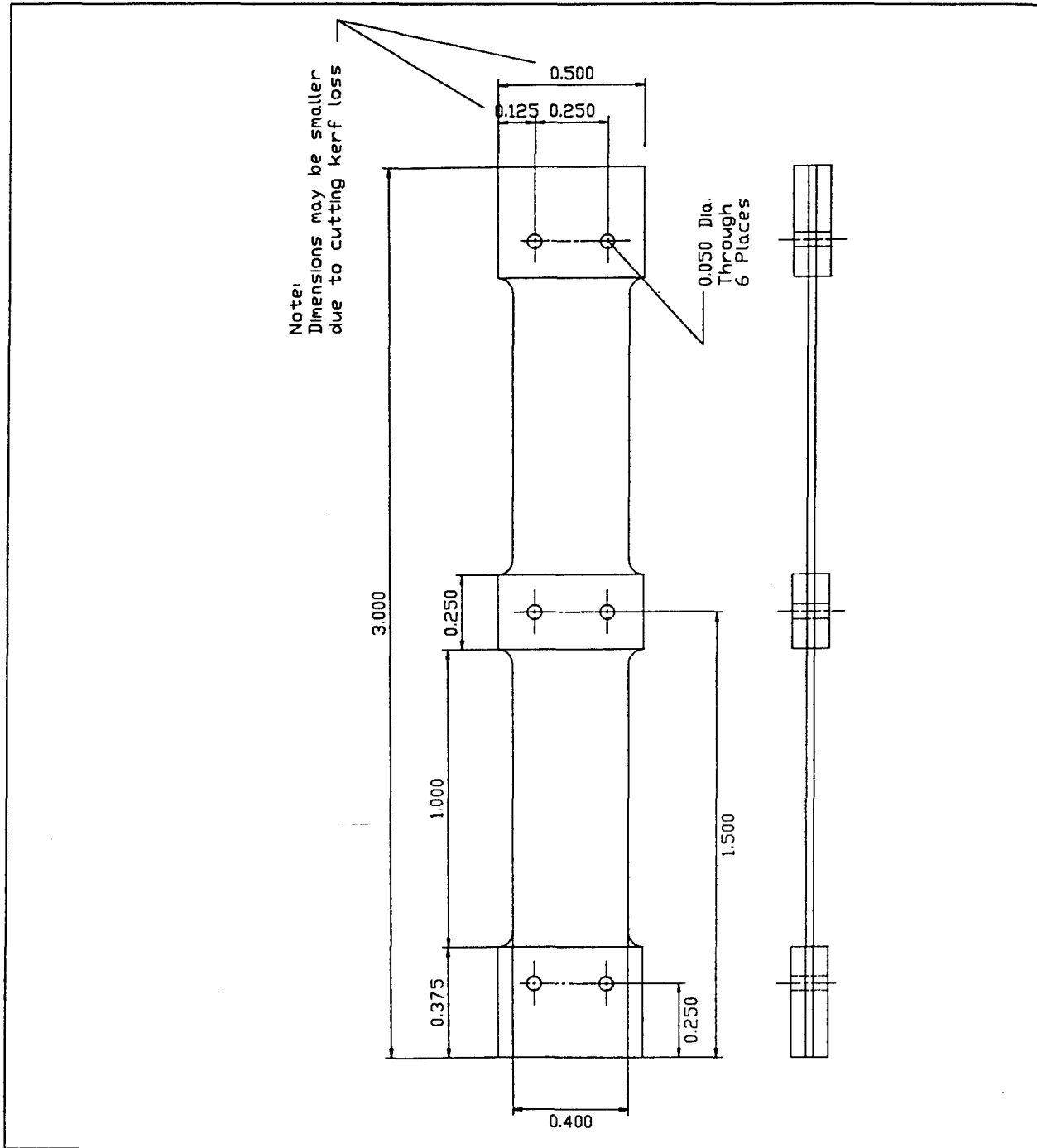
Figure V-6; Fatigue Test Beam Detail

Post Bonding Cut Lines

Plated Surfaces Together

Unplated Surfaces Together

Fatigue Test Coupon (typ)

Doubler (typ)

Flexure Test Beam Bonding/Cutting Assembly
10 Sets of Parts (20 Flexure Beams)
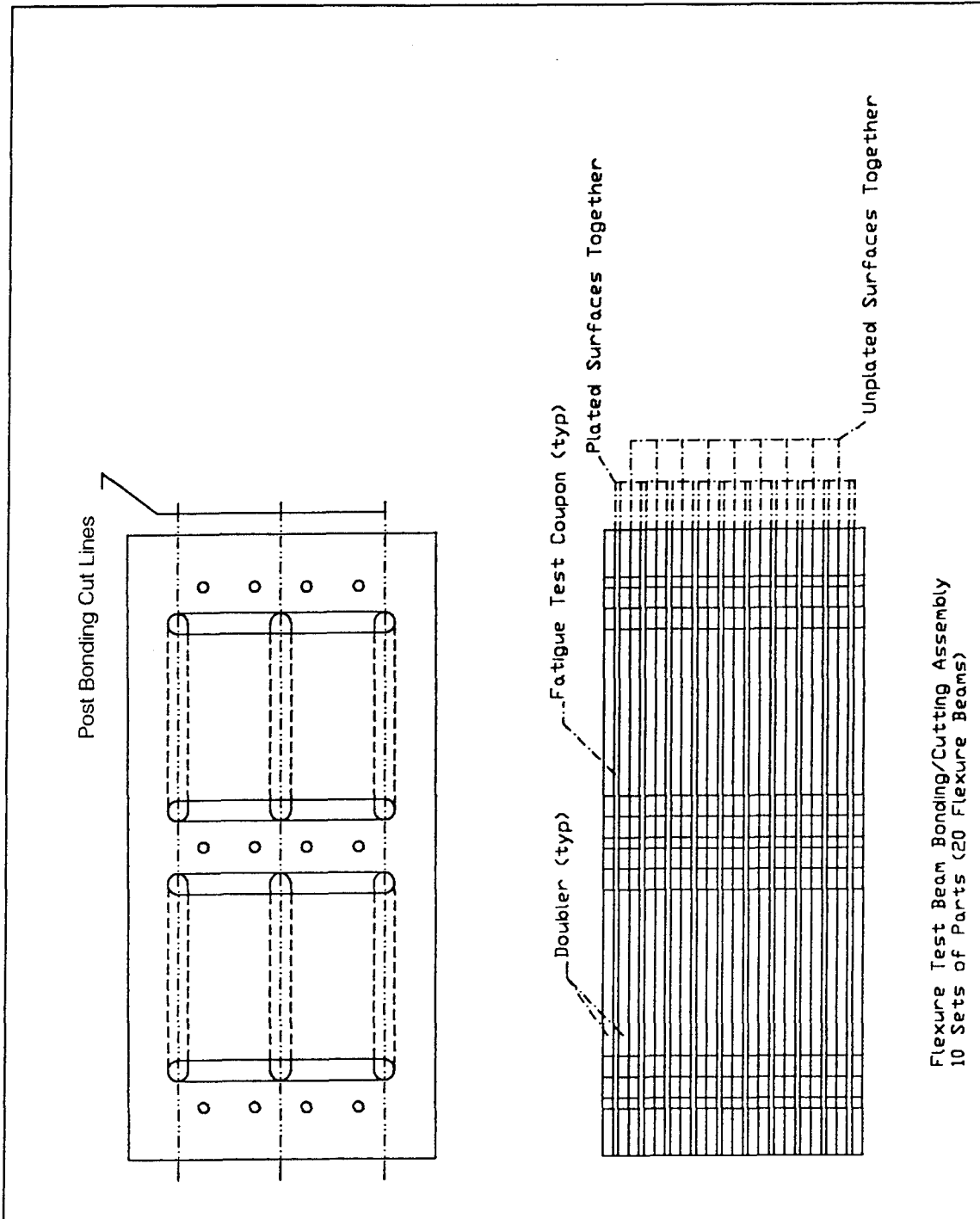
Figure V-7; Diffusion Bonding Stack

Flexure Fatigue Test Coupon, Plated Areas

Material, 0.0100, Uddeholm 716 CRES

Dimensions, 0.000 = +/- 0.0025
0.0000 = +/- 0.0001

Flexure Fatigue Test Coupon Doubler, Plated Areas

Material 0.020, CRES

Dimensions, 0.000 = +/- 0.0025
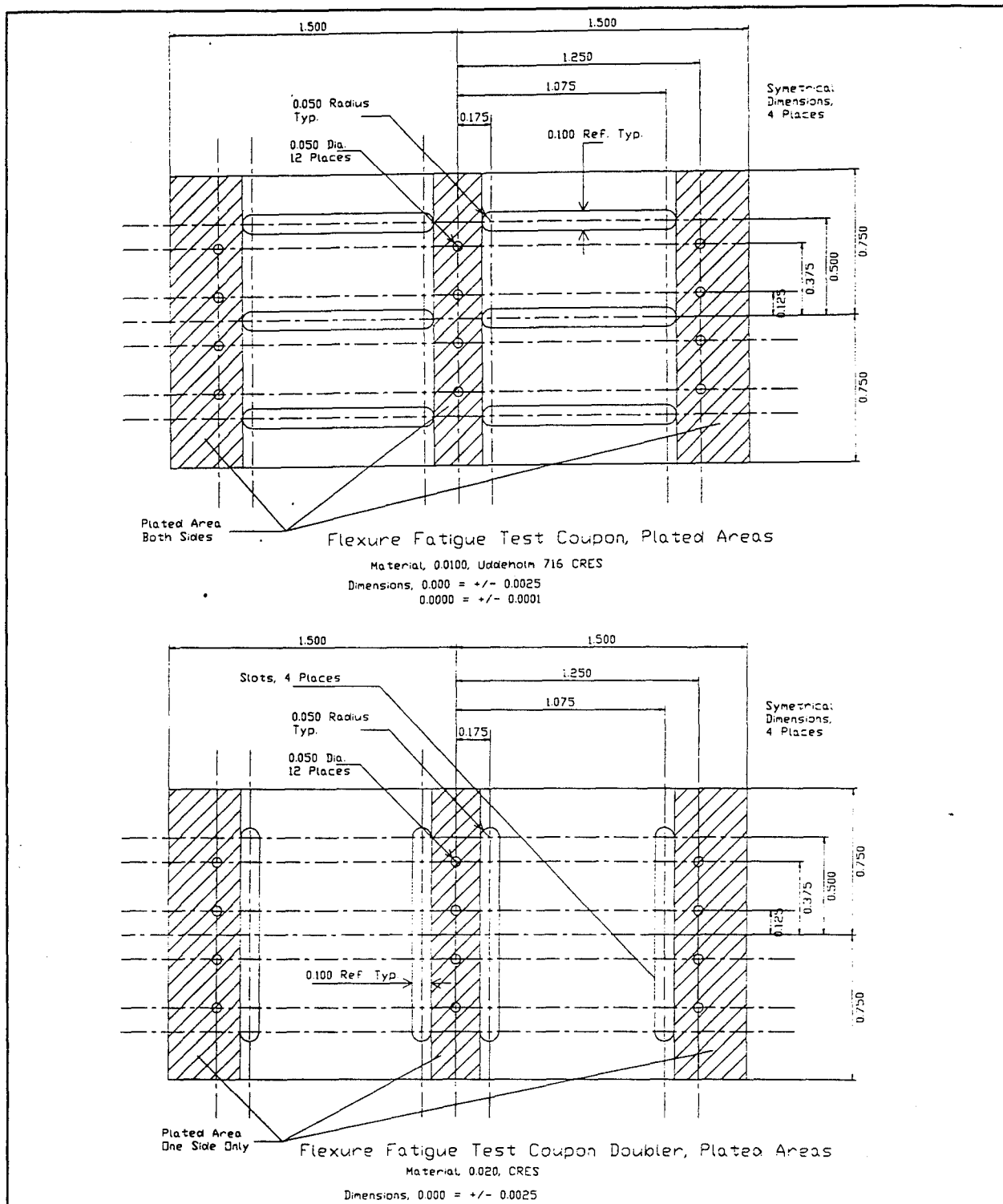
Figure V-8; Fatigue Test Beam Detail Parts

Figure V-9: Unpolished Flexure Edges in Profile and On-Edge
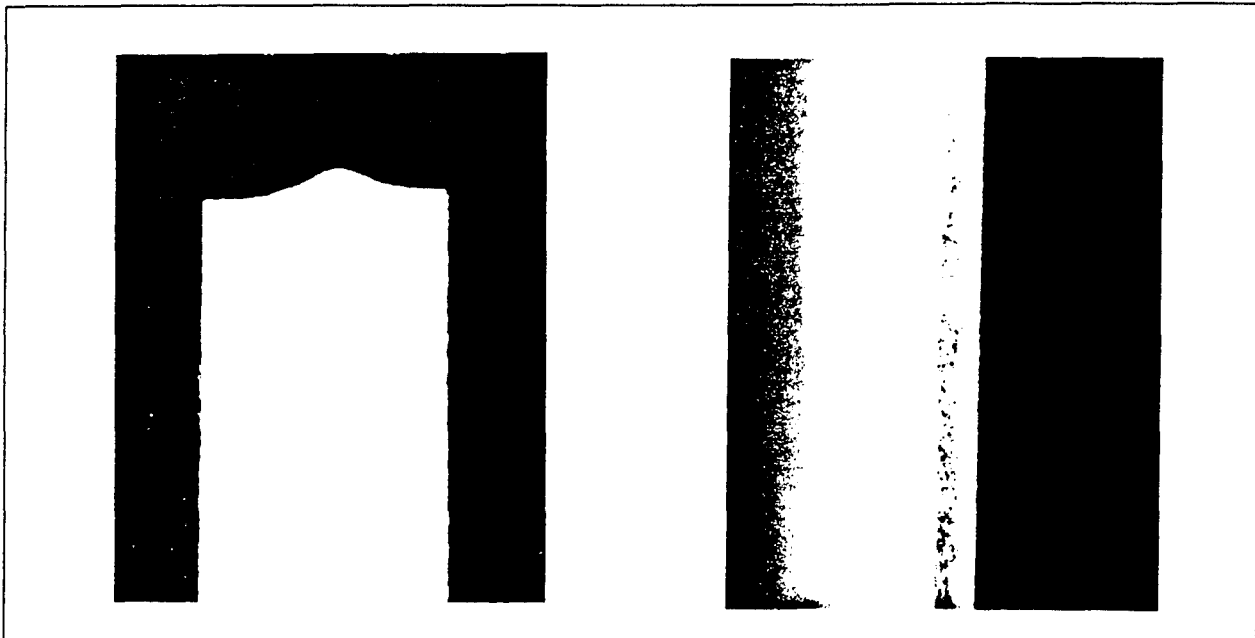
Figure V-10; Chemically Polished Edges in Profile and On-Edge
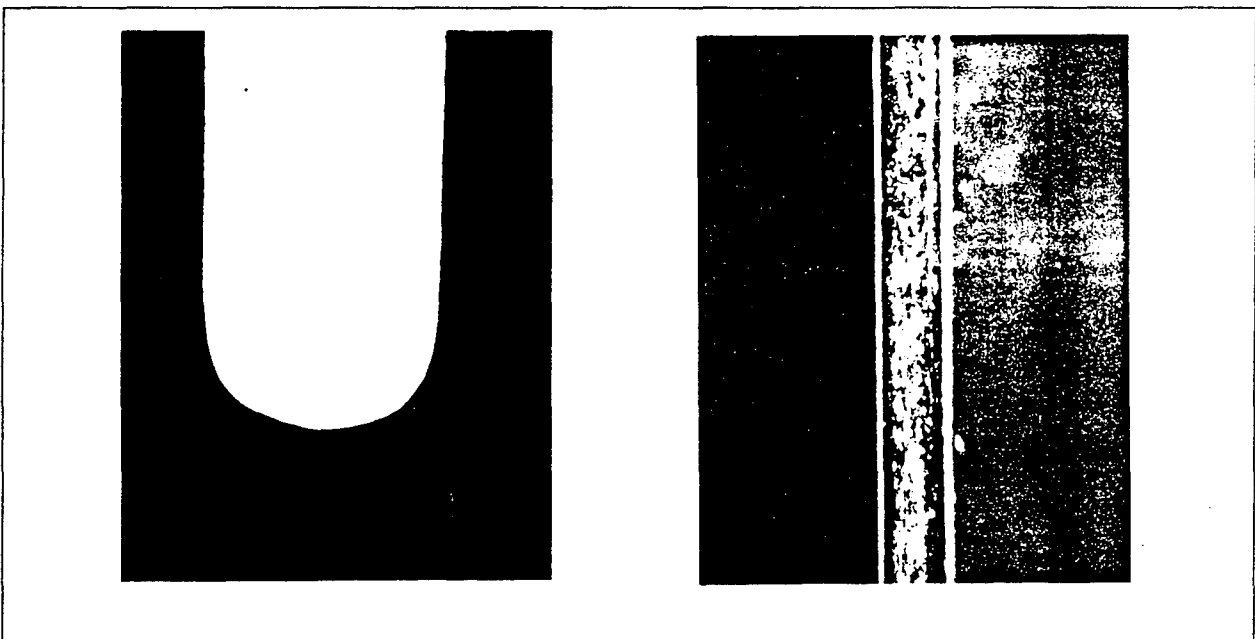


Figure V-11; Mechanically Polished Edges in Profile and On-Edge

## V.5 Fatigue Test Results

Based on the previous analysis, assuming that the flexures are tested within the linear stress range, it is possible to plot the results superimposed on the Uddeholm S-N curves for 716 stainless steel (Figure I-5). The results obtained from the parts fabricated in this Phase I program are presented in Figure V-12. All of the unpolished (photoetched edges) and the chemically polished parts failed and none of the Harperized (mechanically polished) parts failed.
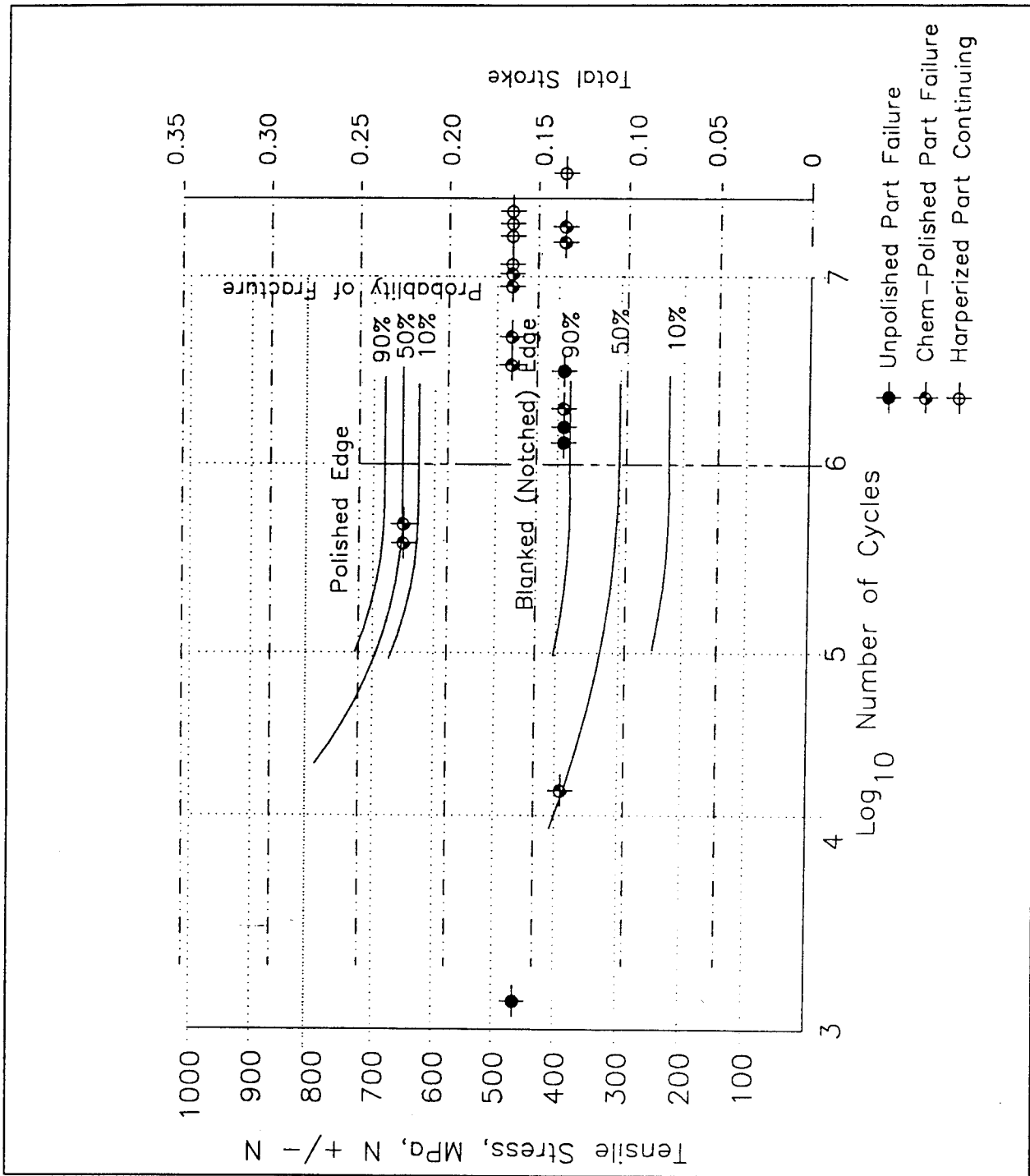
Figure V-12: S-N Data for Diffusion Bonded Uddeholm 716 Stainless Steel Flexure Beams

## VI.0 FINITE ELEMENT ANALYSIS OF FLEXURE BEARINGS

VI.1 Verification of Finite Element Code Predictions

To establish confidence in using a particular finite analysis program for large deflection analysis, a closed-form solution of a simple geometry can be used to verify the accuracy of the computer code. A finite element model of a simple, constant cross-section cantilever beam subjected to end loading perpendicular to the plane of the blade was prepared for this purpose. The predicted deflection and stress distribution was computed and analyzed using Cosmos/M 1.65a. The results corresponded within 1% of the analytical results published by Bisshopp and Drucker[16]. Figure VI-1 depicts the analysis and comparison.

# Verification of Finite Element Code
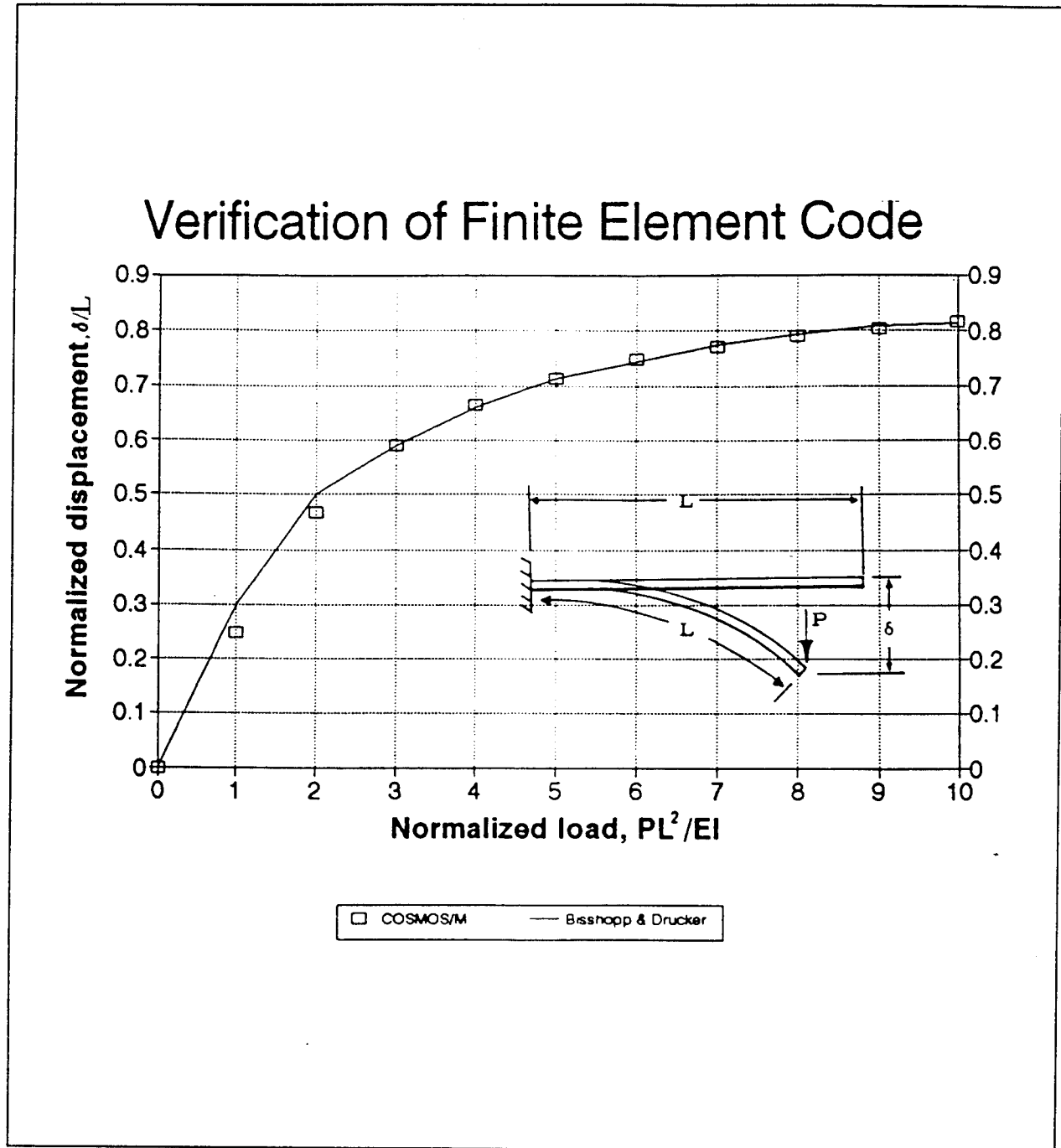


Figure VI-1; Verification of Finite Element Code - Cantilever Beam[16]

VI.2 Comparison Between ABAQUS and Cosmos/M Predictions

The overall dimensions for the circumferential tangential cantilever-cut linear flexure bearing as reported by Wong, Pan, and Johnson[2], together with a typical stress plot produced using the ABAQUS finite element code, were obtained. This information was used to prepare and analyze the characteristics of the Aerospace Corporation (El Segundo, California) design using Cosmos/M. The predictions obtained from the Cosmos M code correlated with those obtained using the ABAQUS code to within 5%. Figure VI-2 presents the overall physical dimensions of the flexure analyzed.
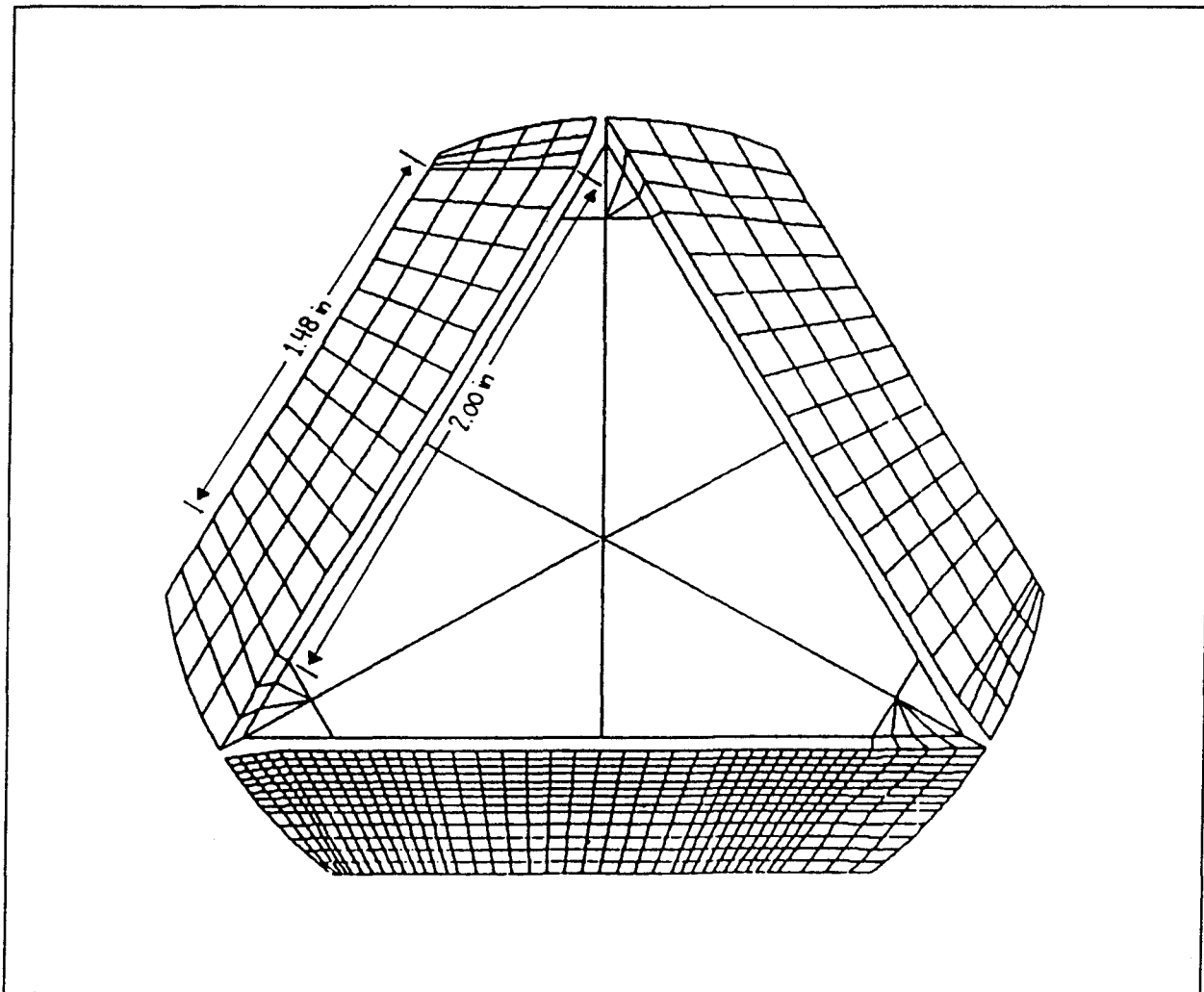


Figure VI-2; Aerospace Corporation Flexure - Finite Element Model

The finite element modeling used for the Cosmos/M analysis is not as finely meshed as that used by Aerospace Corporation for the ABAQUS finite element modeling; however, the results are effectively identical. The finite element meshing selected for the Cosmos/M modeling is based on comparing a number of alternate representations, most of which predicted the same results, but all of which were more time demanding. The Cosmos/M meshing which did not correspond to the ABAQUS results included the extensive use of triangular plate elements in regions of high strain. It was concluded that the use of the triangular element must be limited to noncritical regions of the structure being analyzed. Figure VI-3 shows a typical Cosmos/M result. Table VI-1 presents a comparison between ABAQUS and Cosmos/M results.
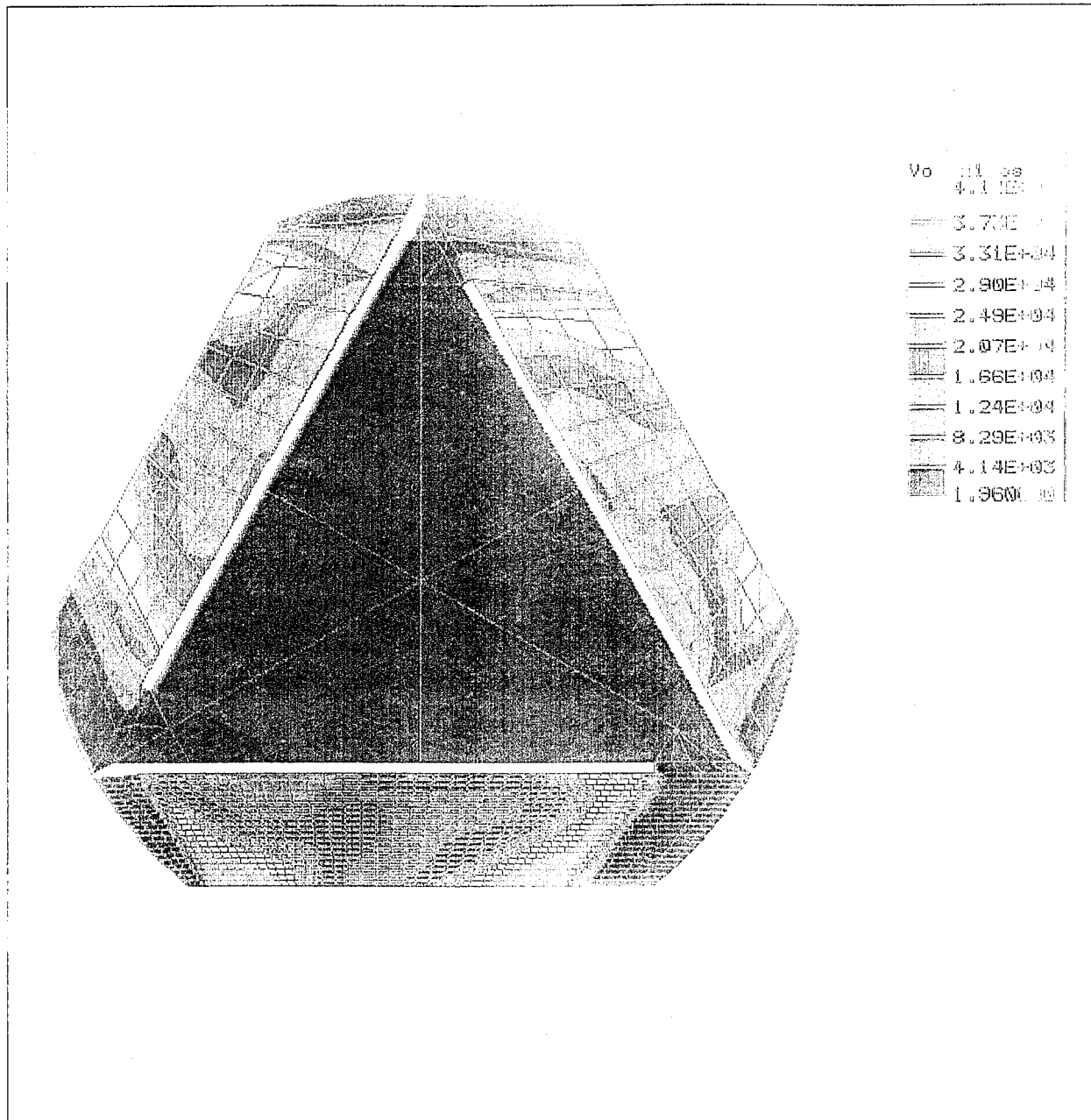
Figure VI-3; Aerospace Corporation Flexure Cosmos/M Model

Table VI-1

Comparison Between ABAQUS and Cosmos/M FEA Predictions

| Code | Axial Stiffness lb/in | Radial Stiffness lb/in | Peak Von Mises Ksi |
|---|---|---|---|
| ABAQUS | 1.66 | 2707 | 44 |
| Cosmos/M | 1.70 | 2709 | 41 |

VI.3  Radial Leg Configuration Characterization

A radial leg configuration flexure was modeled assuming an ID of 2.0 cm, an OD of 10.0 cm, a thickness of 0.025 cm for the flexure portion, a thickness of 0.10 cm per side for the doubler portion, and the geometrical dimensional values shown in Figure IV-4. Using the material properties of Uddeholm 716, the finite element analysis prediction of the radial stiffness, and maximum stress versus axial displacement was prepared using Cosmos/M. From this result, reproduced as Figure VI-5, radial stiffness at a deflection with a maximum stress of 289 MPa was determined.
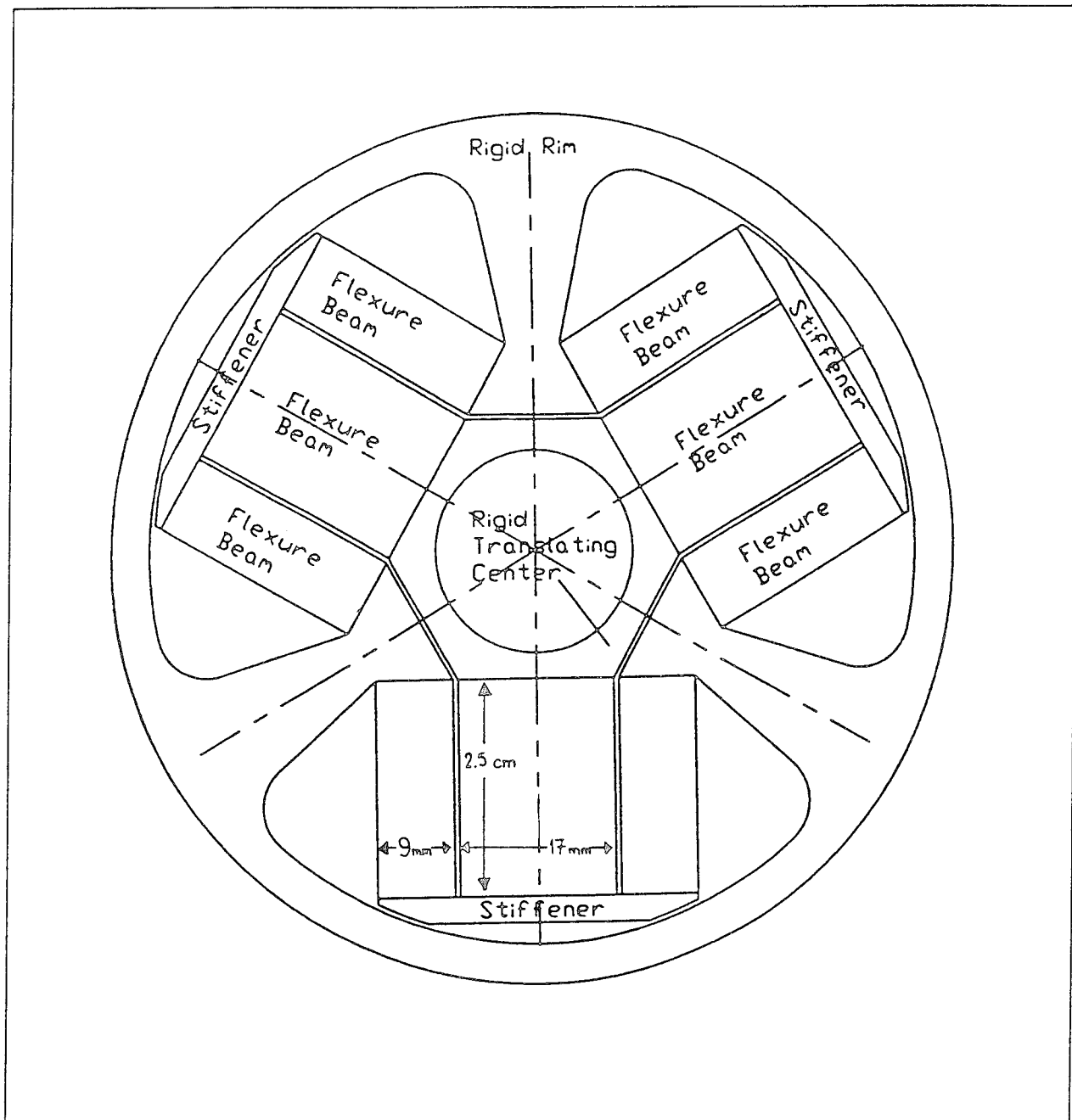
Figure VI-4; Radial Leg Flexure Configuration
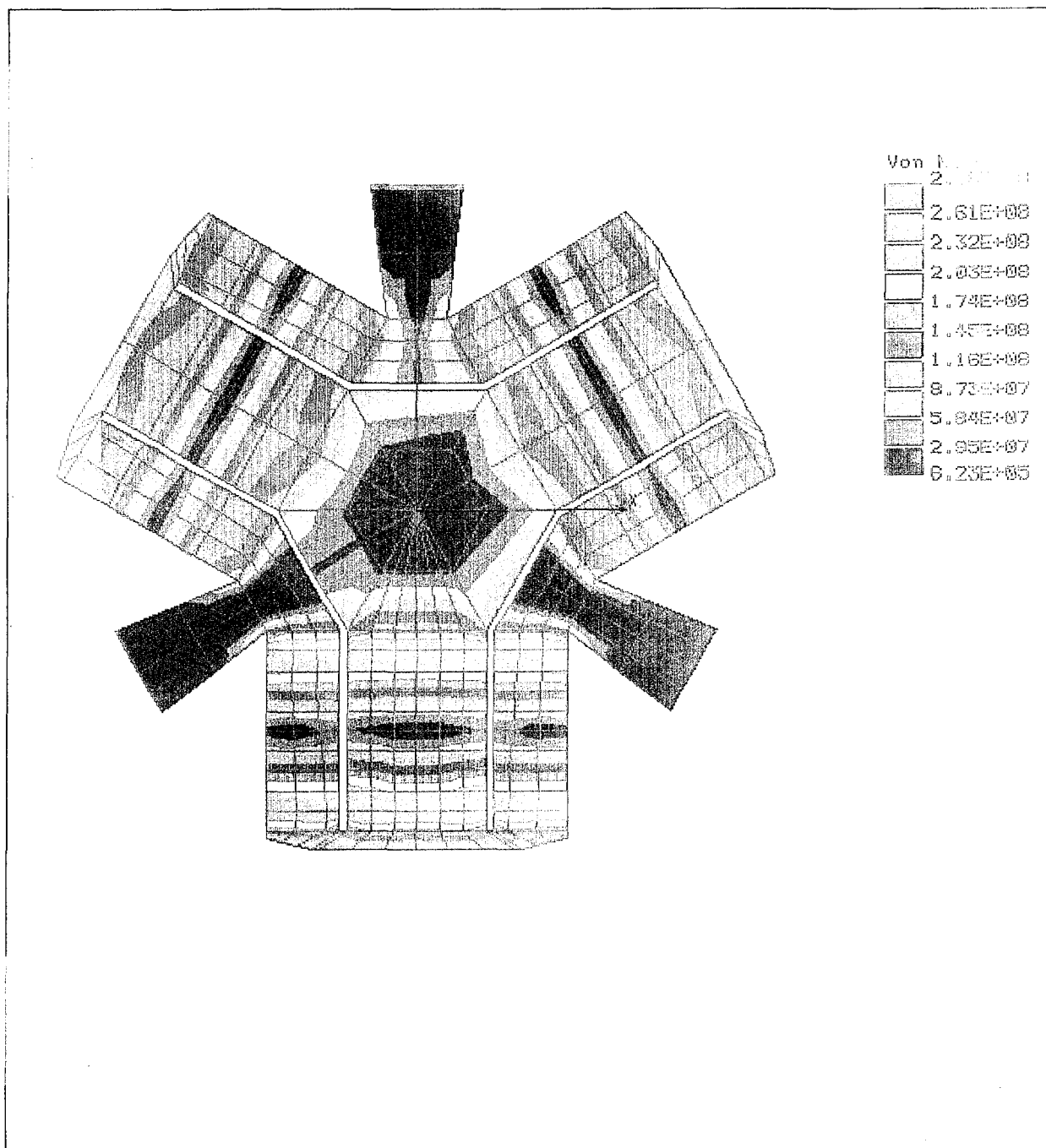
Figure VI-5; Cosmos/M Stress Distribution Plot - Radial Leg Flexure Configuration

VI.4 Characterization of the Tangential 3-Leg Configuration

Assuming an ID of 2.0 cm, an OD of 10.0 cm, a thickness of 0.10 cm per side for the doubler portion, the set of geometrical variables

$\Theta$ = 90°, 105°, 120°
$r_c$ = 0.00 cm
H = 4.25 cm
W = 2.50, 2.00, 1.50 cm
$r_t$ = 0.00 cm
$h_t$=0.025, 0.01875, 0.0125 cm

and the physical characteristics of Uddeholm 716 for the flexure material, a set of predictions of radial stiffness, axial stiffness, and maximum stress versus axial displacement for each configuration was obtained using the Cosmos/M code, Figure VI-6.

For this set of 27 variations, the stress/load response of the selected configuration was obtained using Cosmos/M. Figure VI-7 shows one such typical response characteristic.

Using data such as presented in Figure VI-7, the axial spring rate, the radial spring rate, and the maximum stress versus deflection were computed and plotted. Figure VI-8 shows such a typical plot. From this plotted data, a scatter plot of radial spring rate versus deflection for the maximum stress equal to 0.16 multiplied by ultimate stress was prepared. Based on the Uddeholm quoted value of 1810 MPa for ultimate stress, the maximum "infinite life stress" would be 289 MPa. Figures VI-9, VI-10, and VI-11 show the resultant scatter plot, including the equivalent performance of the flexures analyzed in efforts II and III.
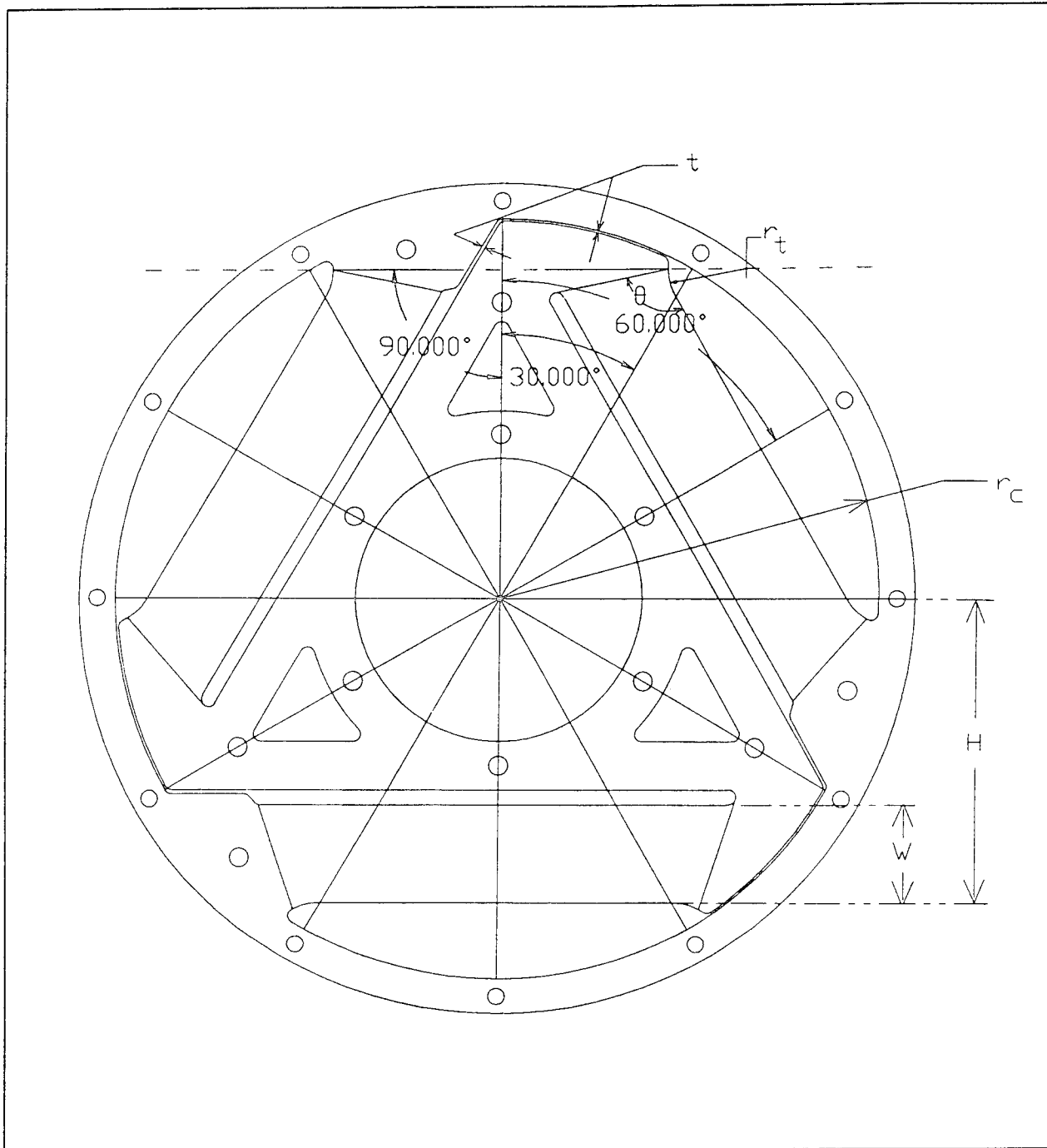
Figure VI-6; Tangential Flexure Geometry
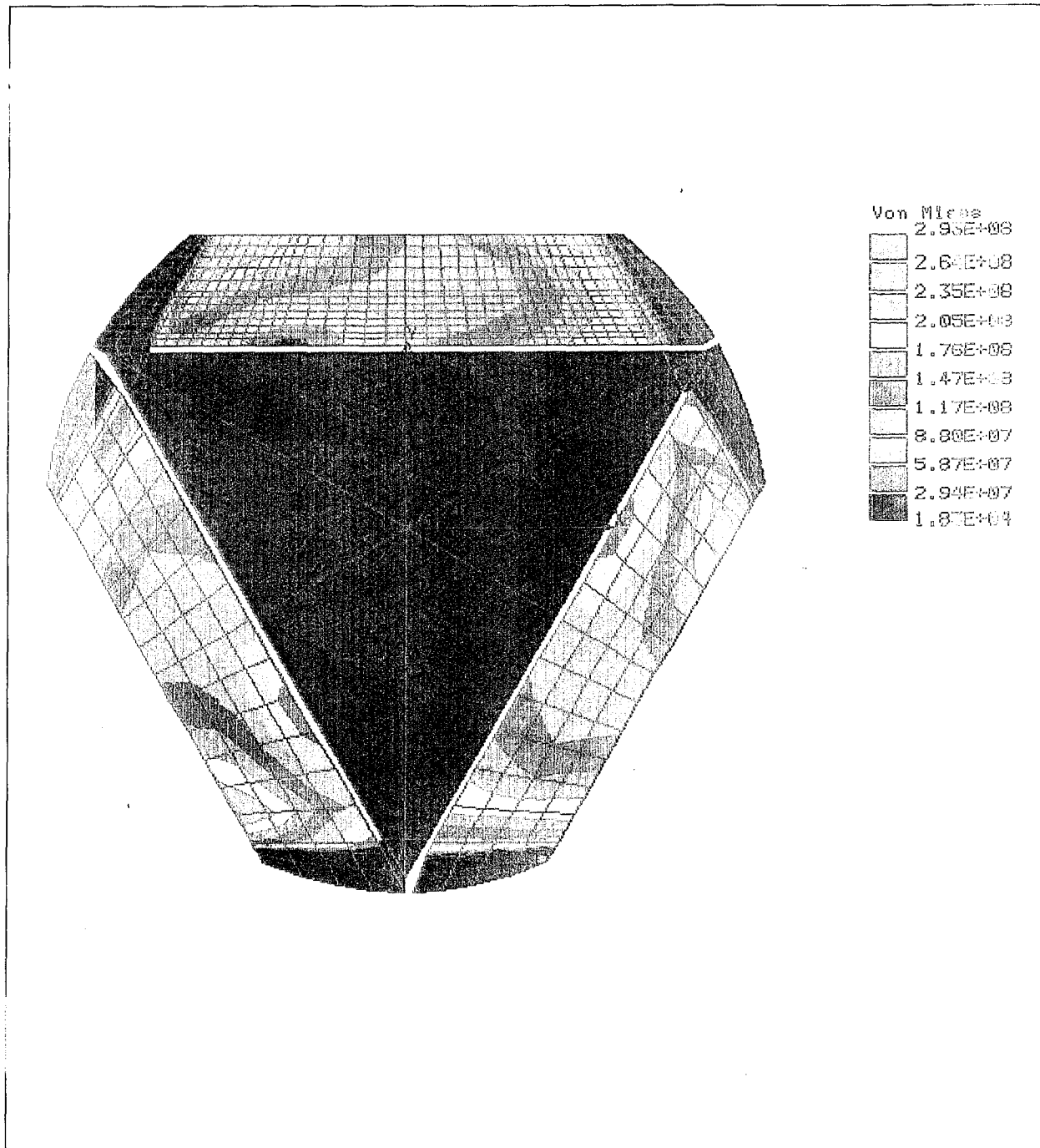
Figure VI-7; Typical Tangential Flexure Nonlinear FEA Stress Plot
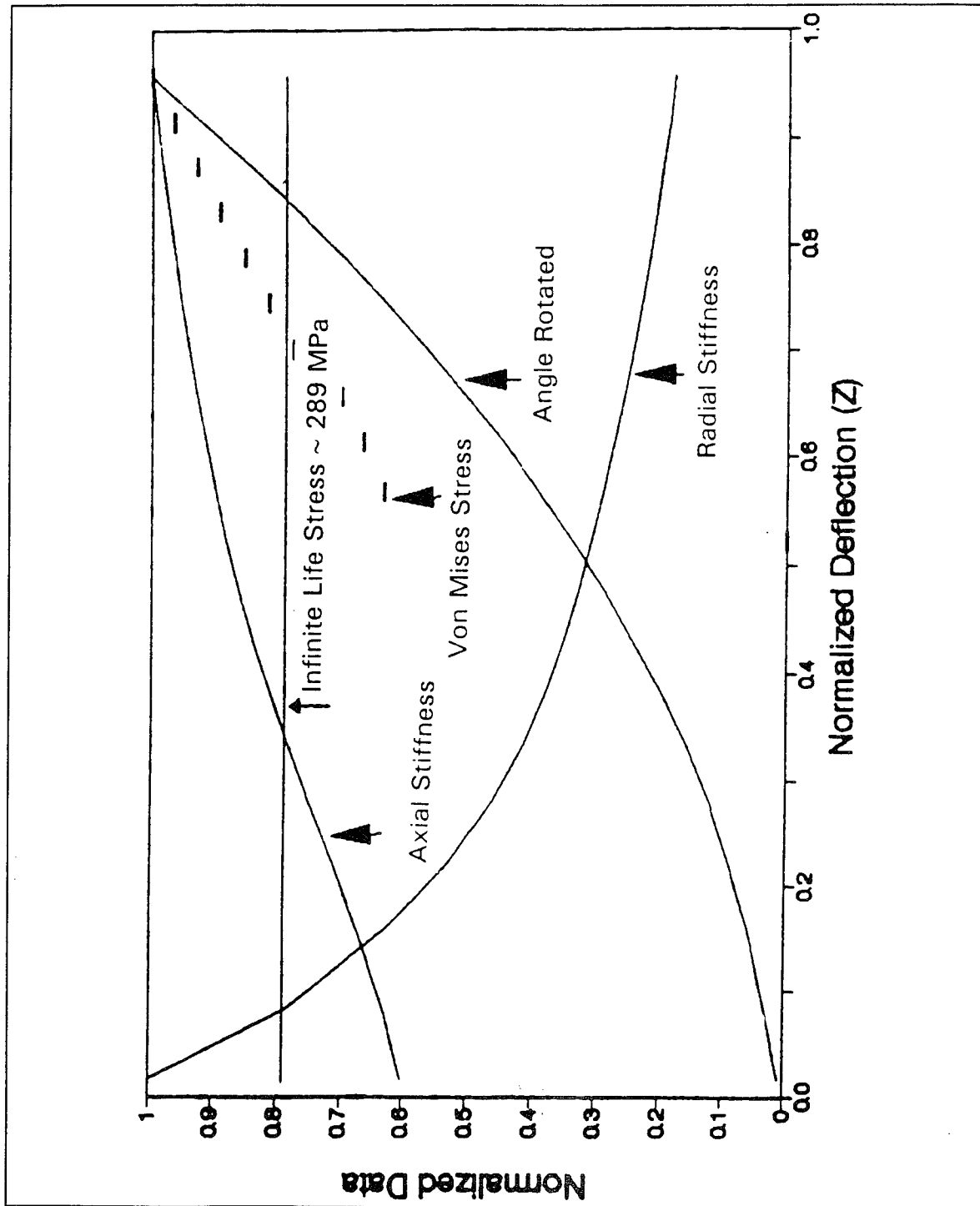
Figure VI-8; Typical Tangential Flexure Characterization Plot (Normalized)

Figure VI-9; Radial Stiffness Versus Displacement - Θ = 90°

# Stiffness (KY) vs Displacement (Z)
## Angle 105

| Code - a b c | a | b | c |
|---|---|---|---|
| | Θ - Angle, degrees | h - Thickness, Cm | W - Width, Cm |
| Value | | | |
| 1 | 90 | 0.0125 | 1.00 |
| 2 | 105 | 0.01875 | 1.25 |
| 3 | 120 | 0.025 | 1.50 |
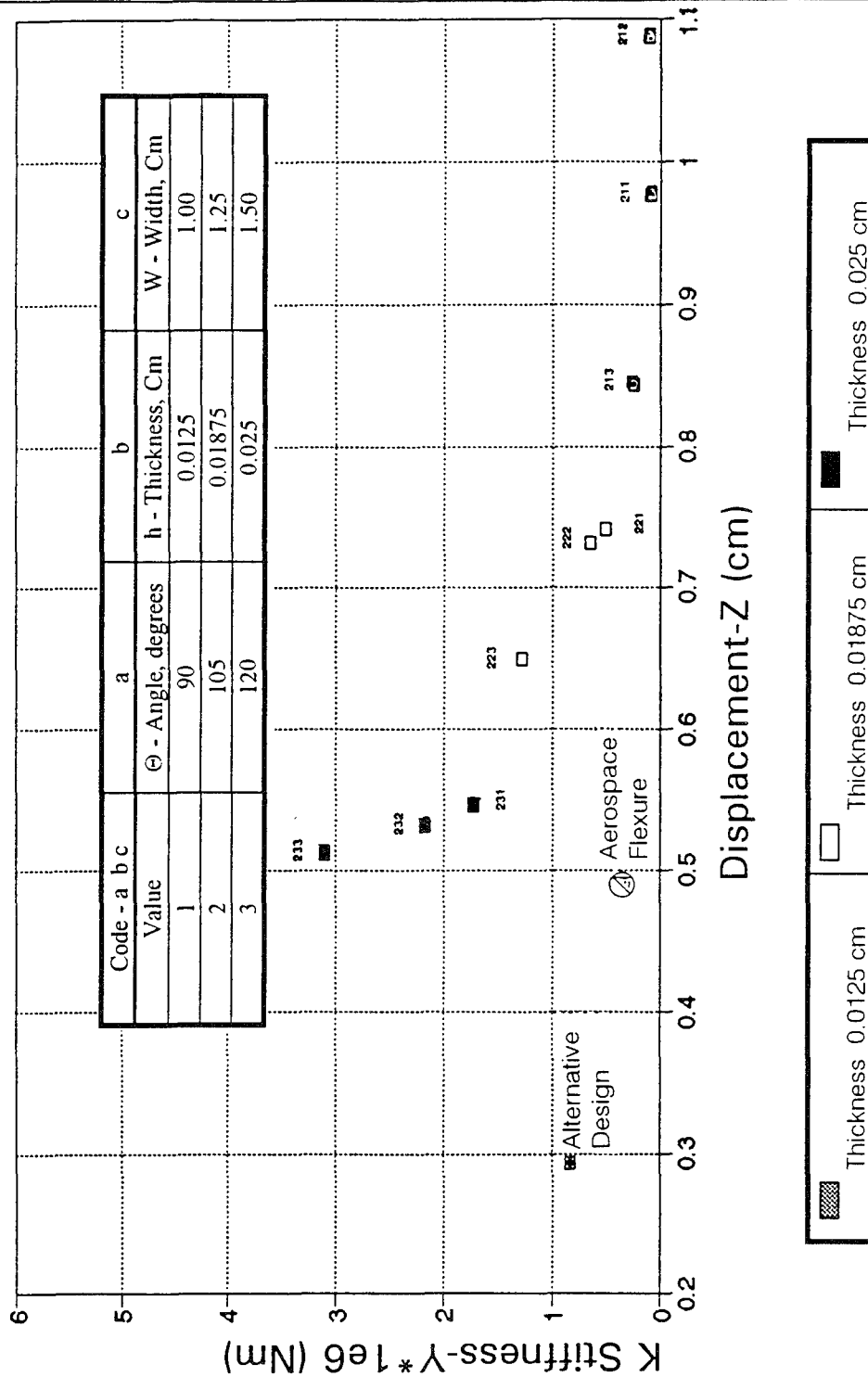
Figure VI-10; Radial Stiffness Versus Displacement - Θ = 105°
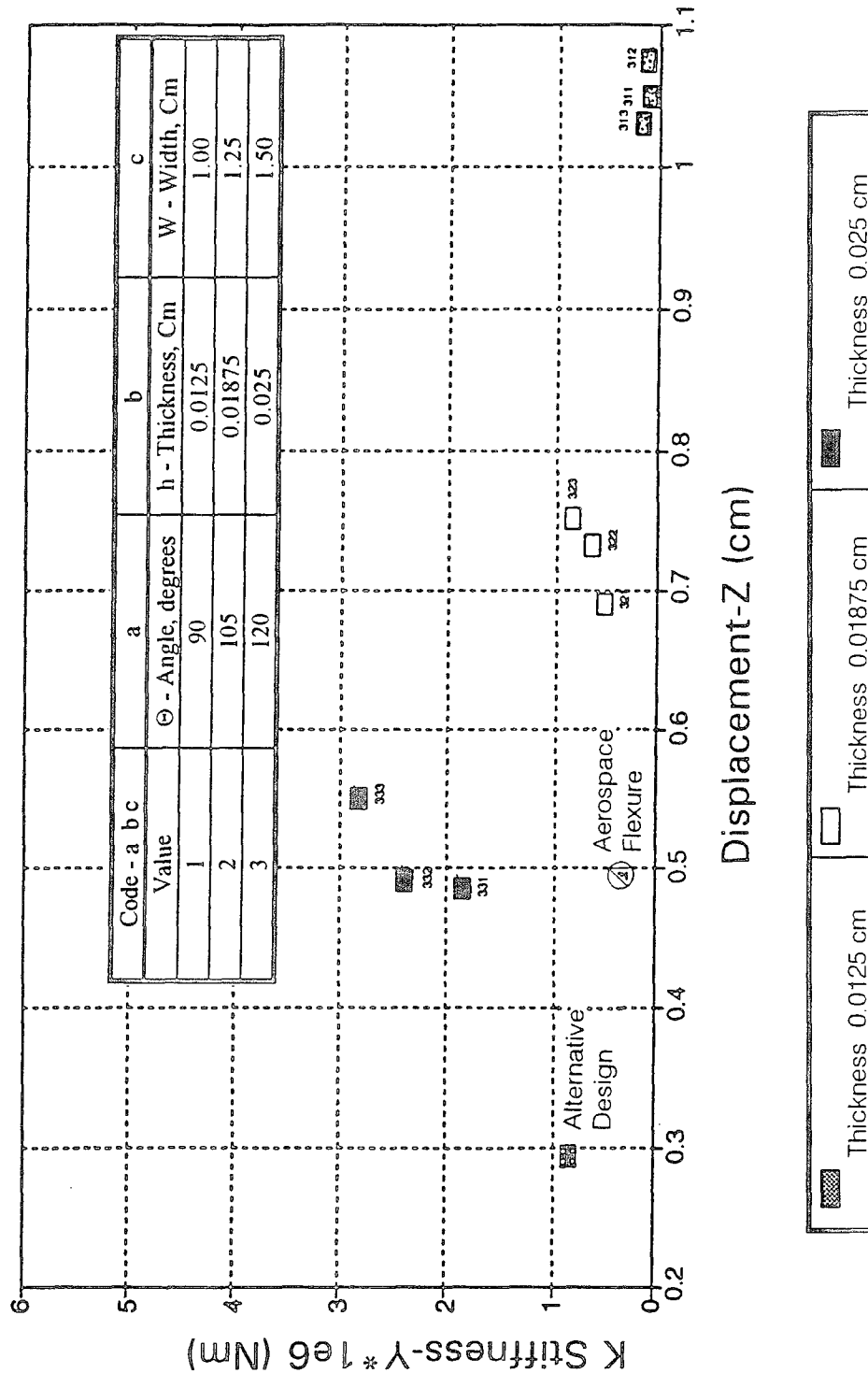
Figure VI-11; Radial Stiffness Versus Displacement - Θ = 120°

## VII.0 RESULTS/CONCLUSIONS

The Cosmos/M finite element code is adequate for predicting the nonlinear characteristics of linear tangential 3-leg flexure bearings.

From an extensive trial and error effort to establish the appropriate Cosmos/M modeling procedures to be used, it was determined that a relatively efficient, relatively low input programming, and reasonably fast computational modeling technique could be used. Based on this effort, it is estimated that the engineering data input effort per configuration analyzed is ~3 hrs per case. The required computational time averaged 4 hrs per case in a PC 486/66 with 16M of RAM and a 210M hard disk. There appears to be no reason to invoke the NIKE3D or DYNA3D capabilities for the Phase II phase, the Cosmos/M capabilities being analytically adequate and cost efficient.

The basic Aerospace Tangential 3-Leg flexure concept is significantly superior to the equivalent form-factor spiral leg flexure. This superiority is ever greater than shown in the initial Aerospace disclosure of this concept[2].

A design manual for the Aerospace Tangential 3-Leg flexure can be prepared as a subtask of the Phase II effort for a reasonable fraction of the total effort.

# References

1.  Johnson, A.L.; "Spacecraft Borne Long Life Cryogenic Refrigeration Status and Trends;" Cryogenics (July 1983)

2.  Wong, T.E., Pan, R.B., Johnson, A.L.; "Novel Linear Flexure Bearing;" Proceedings of the 7th International Cryocooler Conference; Santa Fe, New Mexico (1992)

3.  Marquardt, E., Radebaugh, R.; "Design Equations and Scaling Laws for Linear Compressors with Flexure Bearings;" Proceedings of the 7th International Cryocooler Conference; Santa Fe, New Mexico (1992)

4.  Curtis, P. et al.; "The Pressure Modulator Radiometer for Nimbus F.;" Remote Sounding of Atmospheric Temperature from Satellites; Proceedings of the Royal Society, A 337; London, England (1974)

5.  Davey, G.; "Review of the Oxford Cryocooler;" Advances in Cryogenic Engineering; Volume 35, R.W. Fast, Editor; Plenum Press; New York, New York (1990)

6.  "Servoid Actuator;" South Bend Controls Brochure; South Bend, Indiana (1985)

7.  Johnston, R.P. et al.; "Stirling/Hydraulic Artificial Heart Power Source;" Proceedings of the 12th I.E.C.E.C.; Washington D.C. (1977)

8.  "Fracture Properties of Valve Steels;" Uddeholm Strip Steel AB; Munkfors, Sweden, (Undated)

9.  Tulinski, E.H.; "Centrifugal Barrel Finishing: More Than Precision Deburring and Surface Finishing;" Metal Finishing (July 1993)

10. Spurgeon, W.M., Rhee, S.K., Kiwak, R.S.; "Diffusion Bonding of Metals;" Bendix Technical Journal-Materials and Processing; Volume 2, Number 1; pp. 24-41 (1969)

11. "Shigiya CNC Simultaneous External/Internal Grinder GIE-125;" Shigiya Machinery Works Ltd., Technical Brochure, 92063000 Des Plaines, Illinois (1993)

12. " Practice-orientated universal machines for high-standard workshop;" Studer, Inc.; Technical Brochure 5.92/3000e Bridgeport, Connecticut (1989)

13. Brooktronics Engineering Corporation, 13161 Sherman Way, Unit B., North Hollywood, California 91605 (818) 983-0240

14.   Frahm, H.; U.S. Patent 989,958; <u>Device for Damping Vibrations of Bodies</u>
      (April 1911)

15.   Ormondroyd, J. et al.; "The Theory of the Dynamic Vibration Absorber;" <u>Trans.
      A.S.M.E.</u>, Paper APM-50-7 (1928)

16.   Bisshopp, K.E., Drucker, D.C.; "Large Deflection of Cantilever Beams;" <u>Quarterly of
      Applied Mathematics</u>; Volume III, Number 1 (1945)

# DISTRIBUTION LIST

AUL/LSE
Bldg 1405 - 600 Chennault Circle
Maxwell AFB, AL 36112-6424                              1 cy

DTIC/OCC
Cameron Station
Alexandria, VA 22304-6145                               2 cys

AFSAA/SAI
1580 Air Force Pentagon
Washington, DC 20330-1580                               1 cy

PL/SUL
Kirtland AFB, NM 87117-5776                             2 cys

PL/HO
Kirtland AFB, NM 87117-5776                             1 cy

Official Record Copy

  PL/VTPT/Capt Jeffrey Wiese                            2 cys

Dr. R. V. Wick                                          1 cy
PL/VT
Kirtland, AFB, NM  87117-5776